I. THE FERROMAGNETIC ALLOY SYSTEM COPPER-MANGANESE-INDIUM

II. A VOLUMETRIC METHOD FOR THE DETERMINATION OF INDIUM

Thesis by

Robert Russell Grinstead

In Partial Fulfillment of the Requirements
For the Degree of
Doctor of Philosophy

California Institute of Technology
Pasadena, California
1949

ACKNOWLEDGMENTS

I wish to express my gratitude and sincere appreciation to Prof. Don M. Yost, whose patience and encouragement have guided these, my first steps into the realm of research.

I am especially grateful also to Dr. Thomas L. Allen, who helped construct much of the apparatus and solve many of the problems connected with this research.

Much appreciation is due Prof. Donald Clark and Mr. Osvald Knop for invaluable advice and assistance in the metallurgical phases of this work, and also Prof. Ernest H. Swift and Dr. Eugene Maun for helpful discussions related to the analytical procedures involved here.

Financial aid in the form of a fellowship from the Allied Chemical and Dye Corporation and a grant from the Research Corporation are gratefully acknowledged.

ABSTRACT

A phase-equilibria study of the copper-rich portion of the copper-manganese-indium system has been made, using thermal, microscopic, and magnetic measurements. The thermal data was obtained from cooling curves in the region of solidification, and melting-point contours are given. Microscopic data on the high-temperature solid phases was obtained by annealing the alloys at temperatures just below the solidus, then quenching and observing them under the microscope. The magnetic work consisted of Curie point measurements on the alloys as originally prepared, after quenching, and after reannealing at 100°C. On the basis of these results, approximate locations of the $\alpha/\alpha+\beta$, $\beta/\alpha+\beta$, $\beta/\beta+\beta'$ phase boundaries are given. Ferromagnetism has been found to exist over most of the composition diagram.

An attempt has been made to apply a known method for the volumetric determination of zinc to the determination of indium. The procedure consists of adding an excess of potassium iodide and potassium ferricyanide to a buffered solution of indium, and titrating the liberated iodine with sodium thiosulfate. Within very restricted ranges of concentration, results accurate to ±1% were obtained, but the method is not considered usable at present.

TABLE OF CONTENTS

TABLE OF CONTENTS
(continued)

PART I.

Introduction

Ferromagnetic alloys of the Heusler type have been known for about fifty years. (1) These alloys are interesting because none of their constituent metals are by themselves ferromagnetic. At the present time, several alloy systems as well as some chemical compounds are known to exhibit this phenomenon. (2) The most well known system discovered by Heusler contained copper, manganese and aluminum, and since that time, considerable work has been done on it. (3)(4)(5) In these alloys the magnetism is found to exist in a single phase region, and more specifically, in a region containing an ordered phase, or superlattice. (3)(6)(7) Quite analogous results were obtained with the system Cu-Mn-Sn, (8) this being the only other alloy system which has been extensively investigated. The present research concerns the alloys of copper, manganese and indium which have also been found to be ferromagnetic. (9)(10)(11)

At the beginning of the work, this system had not been reported in the literature. Since in these alloys the magnetism is intimately related to the structure, it was deemed necessary to throw some light on the phase equilibria involved, before proceeding to the study of magnetic properties. As a result, although some magnetic measurements were made, the work has consisted principally of an attempt to locate certain of the phases and their boundaries in this ternary system.

Phase Equilibria Studies

A. Brief Description

The principal source of data consisted of thermal analyses in the form of cooling curves. Alloys were prepared by melting together the desired amounts of the pure metals under argon in a high frequency induction furnace.

Cooling curves were obtained by means of a thermocouple placed in the molten alloy, and the curves were usually continued only through the region of solidification. In the solid state, transitions are difficult to detect and interpret, because both the heat effects and the rates are small, and therefore no systematic attempt was made to record these. Compositions of the alloys were determined by chemical analyses.

The specimens were next annealed at temperatures just below the solidus and quenched to preserve the structure in existence at those temperatures. Information about these structures was obtained by microscopic examination of the quenched alloys.

B. Thermal Analyses

Apparatus: In Fig. 1 is shown the apparatus used in the preparation and cooling curve runs. It is similar to that used by Van Dusen & Dahl (12) in the determination of the freezing points of cobalt and nickel. The furnace consisted of a 61 mm Pyrex tube, open at the top, and with a 35 mm side arm for connection to the vacuum system and a source of inert atmosphere. The top of the tube was closed by sealing to it a Pyrex plate of 2-3 mm thickness with Apiezon sealing wax W.

The vacuum system consisted of a Cenco Megavac forepump and an oil diffusion pump in series. About six feet of 35 mm Pyrex tubing containing one 12 mm stopcock in series connected the oil pump with the furnace. At a point near the furnace tube, a line was run to a mercury manometer and to sources of air, hydrogen, and argon. By proper manipulation of stopcocks, any desired atmosphere could be produced in the furnace. The mercury manometer was used chiefly for the regulation of pressures near one atmosphere.

Heating was done by means of a Westinghouse 10 KW radio frequency generator, operating at a frequency of about 450 kilocycles. Connected to its output terminals was a work coil consisting of ten turns of 3/8" o.d. copper tubing, which fitted snugly around the Pyrex furnace tube for a length of about six inches. The turns of the coil were spaced slightly greater near the center to obtain a more uniform field inside. Cooling water flowing through the coil not only kept the copper cool, but the Pyrex tube as well.

In Fig. 2 are shown the contents of the furnace. Several arrangements were tried; two which were found suitable are pictured. If the alloy was to be heated directly by the R.F. field, the set-up in Fig. 2a was used. The metals were contained in an alundum crucible in which a ceramic thermocouple tube was placed. This tube was packed for a length of about one centimeter with powdered magnesia and rested on the bottom of the crucible. Enough metal was taken to give a depth of at least 3 cm. when molten. Alundum discs served as crucible covers and as weights to prevent the molten alloy from floating the hollow tube. The remainder of the space was filled with powdered zircon or zirconia, except for a small alundum tube which extended from the top of the crucible to the surface of the powder. To prevent convection currents in the air space above the contents a set of asbestos or mica disks, with Pyrex spacers, was used.

In some cases it was found advisable to use the apparatus in Fig. 2b where only the inner Pyrex tube is shown. The essential difference in the two arrangements is that in the latter a graphite or steel crucible surrounded the alundum one, so that the heat was generated in the outer crucible. A cover of graphite or steel was also used, on top of which a zircon disc was placed for insulation.

Great difficulty was experienced in obtaining crucibles of satisfactory size and material. No difficulty is encountered with copper or indium, but manganese reacts with silica (8) and also forms a carbide, (8) so that graphite and quartz cannot be used. Basic oxides such as alumina and magnesia are satisfactory (13) and zirconia was also found suitable. However, zirconia crucibles of the desired size and shape were difficult to obtain. Therefore, attempts were made to prepare zirconia crucibles by slip-casting. (14) Zirconia powder was obtained from the Titanium Alloys Manufacturing Company and made into a slip or suspension with 2% sodium pyrophosphate. The slip was poured into two-piece plaster of paris molds which quickly extracted water from the slip. Upon pouring out the excess slip, a smooth coating of zirconia was left on the walls of the mold. As the dehydration process continued the mass shrunk from the walls and could be gently removed. The crucibles were then dried at temperatures of a few hundred degrees centigrade and used. Facilities for sintering were not available, and the crucibles were of limited use, since they were quite brittle and somewhat porous. However a few alloys were prepared in them with success.

It was eventually discovered that alundum extraction crucibles, manufactured by the Norton Abrasive Company were of about the desired size and shape. The densest of these, porosity grade RA 84, dimensions 90 x 19 mm., was found to work fairly satisfactorily, though the porosity caused the loss of a few percent of the manganese and indium during the preparation and cooling runs.

Thermocouple tubes were obtained from the Stupakoff Ceramic Company, and were made of alumina and some silica. The silica present did not appear to cause any trouble, perhaps because it was in combination with the alumina. These tubes had an outside diameter of 4.75 mm., and a wall thickness of about .5 mm.

Temperature measurements were made with 28-gauge chromel-alumel thermocouples. The two wires were melted together, threaded through a two-hole porcelain thermocouple insulator, which fit snugly down inside of the protection tube. The wires were led out of the furnace tube through two small notches at the top where the Pyrex plate was waxed onto the tube, thence to a cold junction and a cable terminal.

The measurement of the emf of the thermocouple was made in two ways. One method was by means of a Leeds and Northrup type K potentiometer, using a galvanometer of 1681 megohms sensitivity for the null indication. The sensitivity of this instrument was reduced by shunting so that a movement of one cm. on the light scale corresponded to a temperature change of about one degree centigrade. Later in the work, a Brown Continuous Balance Potentiometer Recorder was obtained; this instrument performed very satisfactorily and eased considerably the job of running the cooling curves. A 500-1200°C. scale was used, and it was operated from the same thermocouples as the potentiometer. A self-compensating circuit which corrected for the room temperature was contained within the instrument. This feature necessitated removal of the cold junction and making the entire thermocouple circuit of chromel-alumel wire, so that the effective cold junction would be on the terminal block inside the case containing the compensator.

The Brown Potentiometer recorded the temperature on a moving chart, resulting in automatic drawing of the cooling curve. A variety of chart speeds was available, so that the shape of the curve could be made optimum.

Couples 1 and 2 were calibrated by comparison with a platinum—10% platinum-rhodium couple. This couple had been previously calibrated by Don S. Martin, Jr., using Bureau of Standards zinc and lead, 99.8% pure antimony, and boiling water. The comparison was carried out in the annealing furnace, a description of which is given in a subsequent section. In order to insure that the hot junctions were at the same temperature, they were inserted in quartz tubes and bound together with copper sheet for about two inches on either side of the junctions. Simultaneous emf readings were taken of the couples, the temperature in each case being allowed to come to a nearly constant value before readings were made. Four points were recorded in this manner from 0° to about 900° C. In the case of couple No. 1, which was used in cooling curve runs, two additional points were determined, one at the freezing point of Bureau of Standards copper, a second at the freezing point of some $99.8^{+}\%$ pure antimony. The impurities were estimated not to lower the freezing point more than about two degrees C., and since the freezing curve was very flat, the antimony was considered suitable for a calibration point. The copper freezing point was determined in the regular cooling curve apparatus, while that of the antimony was done in a graphite crucible in a simple electric furnace, using a layer of powdered graphite for protection from oxidation.

Couple No. 2 was used in the annealing furnace and was not calibrated further. Couple No. 4 was used for a few cooling curve runs in the region of 600°-700° C., and was checked only at the antimony point.

Conversion tables published by the National Bureau of Standards (15)(16) were used in the construction of error curves for the couples. The conversion table for chromel-alumel couples is reproduced in Table I, and in Table II is shown the calibration data. An additional correction, not indicated in the table, was applied to take care of an inconsistency among the potentiometers. The high scale of the type K instrument was found to check to within one degree Centigrade with the Brown indicator and was therefore used as a standard. The low scale, in which the variable resistance was all contained in the slidewire, was then found to read low by 0.28 millivolt per 100 millivolts. The student potentiometer had a constant error, on this basis, of -1° C. on

TABLE I

Temperature-emf Conversion Table for Chromel-alumel Thermocouples

(emf in millivolts)

°C. Temp.	0	10	20	30	40	50	60	70	80	90	100
0	0.00	0.40	0.80	1.20	1.61	2.02	2.43	2.85	3.26	3.68	4.10
100	4.10	4.51	4.92	5.33	5.73	6.13	6.53	6.93	7.33	7.73	8.13
200	8.13	8.53	8.93	9.34	9.74	10.15	10.56	10.97	11.38	11.80	12.21
300	12.21	12.62	13.04	13.45	13.87	14.29	14.71	15.13	15.55	15.97	16.39
400	16.39	16.82	17.24	17.66	18.08	18.50	18.93	19.36	19.78	20.21	20.64
500	20.64	21.07	21.49	21.92	22.34	22.77	23.20	23.62	24.05	24.48	24.90
600	24.90	25.33	25.75	26.18	26.60	27.03	27.45	27.87	28.29	28.72	29.14
700	29.14	29.56	29.98	30.40	30.82	31.23	31.65	32.07	32.48	32.90	33.31
800	33.31	33.71	34.12	34.53	34.94	35.35	35.75	36.16	36.56	36.96	37.36
900	37.36	37.76	38.16	38.56	38.96	39.35	39.75	40.19	40.53	40.92	41.31
1000	41.31	41.70	42.08	42.47	42.86	43.24	43.62	44.00	44.38	44.76	45.14
1100	45.14	45.52	45.89	46.27	46.64	42.01	47.38	47.75	48.12	48.48	48.85
1200	48.85	49.21	49.57	49.94	50.29	50.65	51.00	51.36	51.71	52.06	52.41
1300	52.41	52.75	53.10	53.45	53.79	54.13	54.47	54.81	55.15	55.48	55.81
1400	55.81										

TABLE II

Thermocouple Calibration Data

True Temperature °C.	emf Equivalent (mv)	Corrections for couple in (mv)				Remarks
		#1	#2	#3	#4	
82	3.34		-.07			Comparison
200	8.28	-.15	-.11			Comparison
327.4	13.34				-.07	F.P. of NBS Lead
444	18.37	-.12	-.05			Comparison
630.5 *	26.20	+.06		+.10		F.P. of 99.8% Antimony
670	27.88	-.01	+.13			Comparison
904	37.37	+.15	+.40			Comparison
1083 *	44.49	+.57				F.P. of 99.9% Copper

* Although these were not NBS samples, errors due to F.P. lowering should be less than 2° C.

the low scale and -4° C. on the high scale. A further correction was made in the case of a few alloys which were run with the Brown potentiometer. A chart error sometimes occurred, due to changes in temperature or humidity which caused the chart and pointer to give different readings. These corrections were applied to all results obtained on the potentiometers. The couples thus calibrated should have an accuracy of at least ± 3° C.

The charts and scale of the Brown potentiometer had been prepared using the same conversion table, and the instrument had a guaranteed accuracy of ±.25%. As mentioned above, a comparison with the type K potentiometer showed agreement to within at least one degree Centigrade over the whole range.

Materials: Indium of purity 99.97% was obtained in the form of small pellets from A. D. Mackay and Company of New York and from the Indium Corporation of America. #16 gauge copper wire was obtained from the Malin Wire Company and was said to assay greater then 99.9% copper. The manganese was obtained as small plates from A. D. Mackay and from Mr. C. W. Davis of the U. S. Bureau of Mines. Both lots were said to have a purity of 99.9% or better. Melting points of the copper and of the manganese obtained from Mackay were measured, using a Leeds and Northrup optical pyrometer. The pyrometer was calibrated by Leeds and Northrup and found to be accurate to ± 3° C., but on the basis of the measurement of melting points of two samples of copper, which gave flat freezing curves and identical freezing temperatures, was probably 2-3° C. low. The runs made in the cooling curve apparatus, the pyrometer being sighted down the thermocouple tube. The correction due to the glass plate was determined by sighting on a 100 watt bulb first through the plate and then without the plate. Very flat freezing curves were obtained for both metals, the copper freezing at an observed value of 1080° C. and the manganese at 1242° C. Pure copper melts at 1083° C. (17) and 99.99%

pure manganese at about 1242° C. (13) It has been estimated (17) that the melting point of copper may be lowered as much as .1° C. by .01% impurities, so that .1% impurity could cause a 1° C. lowering. The freezing point of manganese is sometimes raised by impurities so it is not possible to estimate as easily the effect of impurities. However, on the basis of the close agreement with known values of the melting points, the metals were considered to be sufficiently pure for further work.

Preparation and cooling runs: The alloys were prepared at first by weighing out the desired quantities of metal to 10 milligrams and placing them in the crucible. A total of 50 grams was used for each preparation. Analyses showed that manganese and indium were being lost during the runs, in quantities of the order of one or two atom percent of the total. Subsequent weighings were therefore done to 0.1 gram on a pan balance, and the exact composition obtained later by chemical analysis. The sample was sealed into the furnace and the whole system was evacuated with the forepump for about half an hour. Argon, obtained from the Linde Air Products Company, with a reported purity of 99.8%, was let in at a pressure of one atmosphere, and heating was begun. Hydrogen and nitrogen could not be used, since both react with manganese. (18) Helium was used for a while, but it was thought that argon would be less easily absorbed in the melt.

It was found to be desirable to heat the metals above the melting point of the manganese for about a half hour to ensure mixing, rather than to rely on solution of the manganese in the copper-indium melt. At first the system of Fig. 2a was used, but owing to the fact that heat is generated non-uniformly in the various sized particles, some manganese would usually become wedged in the upper cooler portion of the crucible and remain unmelted. In addition, the alloys would turn out with an external film of greenish substance, presumably an oxide of manganese. According to Mellor, (19) the oxide MnO is emerald green, and in certain proportions, mixtures of MnO and Al_2O_3 are the same color. (20) It thus appears that traces of oxygen were responsible for the film. The coating appeared to be merely a surface one and could easily be ground off.

In an attempt to prevent this film, the crucibles were heated to 1000° C. in hydrogen and then pumped on to remove any oxygen adsorbed on the walls. They were cooled in argon, immediately filled with metal and replaced in the system. This procedure did not seem to have any effect and was given up. Pumping with the aid of the oil diffusion pump for several hours, or overnight, gave an improvement, but a better scheme was sought. The trouble was apparently due to the manganese, since copper-indium binary alloys, and also the pure metals, were always clean-appearing upon removal from the system.

Melting of the metals was subsequently carried out using the scheme of Fig. 2b. Here the graphite or iron crucible served to maintain a more even temperature around the whole crucible and the alloys were easily melted. Especially in the case of graphite, no trouble was encountered with surface oxidation, and the alloys could be prepared quite clean in appearance. The oxides of manganese have higher heats of formation than oxides of copper, hydrogen, iron or carbon; however, the graphite apparently prevented the traces of oxygen from reaching the metals, and so prevented the formation of the manganese oxide.

This new arrangement was therefore a great improvement but had the disadvantage that mixing was not complete, even after a half hour of heating at 1250°-1300° C. and 2 or 3 hours above 1100° C. When heated directly by the R.F. field, eddy currents are set up, which mix the metals thoroughly.

This phenomenon has been noticed before (21) and can be observed by melting a metal in a crucible without a cover. To obtain homogeneous alloys using the graphite and steel cylinders, the first melt was crushed, mixed, and remelted a second time. This procedure gave good results except in the case of some of the softer alloys which could not be crushed, and had to be sawed or broken up into smaller pieces.

The cooling curves were then run using the external graphite crucible rather than the steel one, since steel was known to show thermal effects in the vicinity of its Curie point (about 785° C.) and possibly also at other temperatures.

Using this last method, the first melting was done at about 1250°-1300° C. for 15-20 minutes, then at 1100° C. for about two hours. The second melting was done at 1100° C. for about half an hour, after which the alloy was allowed to cool slowly.

In the presence of an atmosphere, the heat losses were so great that the cooling rate was much too fast to obtain good curves. In a vacuum the cooling rate was satisfactory, but the danger of losing manganese by distillation prevented the use of this procedure. It was found that by reducing sufficiently the power output of the R.F. generator, any desired cooling rate could be easily obtained, and this procedure was used throughout the experiments. Line voltage fluctuations would be expected to give difficulty but did not do so. The variations in generator output were long term ones, and over the course of a half hour or an hour were so small as to be unobservable. To make sure of this, however, and also to make certain that complete mixing had occurred, two or more cooling runs were made, and the sample heated for an hour or so in the meantime. At the beginning of the runs, the cooling rate was adjusted to about 10° or 12° C. per minute, although rates as high as

25° C. per minute and as low as 7° C. per minute were used. In some cases, two successive runs on the same alloy were made with different cooling rates, in order to determine whether the rates were sufficiently slow. With rates of the order of those mentioned above, no significant difference was ever observed. Another check on the rates was afforded by the calibration run on copper. Few alloys melted as high as 800° C., yet copper, melting at 1083° C., gave a freezing curve which was quite flat and had sharp breaks at both ends of the plateau. The sharpness of the breaks can be taken as an indication of the quality of thermal contact between couple and sample. Nearly all samples gave sharp breaks at the beginning of precipitation of a phase, though the endings were usually uncertain, due to reasons to be discussed in a later section.

The effect of the R.F. field on the thermocouple does not need to be considered since the junction and part of the lead wires are shielded by the sample itself. The heat is generated in a thin layer in the outer circumference of the alloy or of the graphite crucible, if one is used. Some heat may be generated in the lead-in wires above thetop of the crucible, but this should have only the effect of supplying some of the heat losses through these wires.

During the runs in which the potentiometer was used to record temperature, simultaneous readings of a stopwatch and the potentiometer were recorded. After some experience with the procedure, readings could easily be taken every 15 seconds, a speed which, upon plotting the data, was seen to be ample to determine the position and duration of breaks in the curve. When the Brown recorder was used, the curves were then drawn automatically. After the cooling runs were finished, the alloy was remelted and the R.F. generator turned off. Thus, cooling through the solidification region would be accomplished quickly and segregation would not be as likely to occur. In the cooling run of A9, the Leeds and Northrup student potentiometer was used, the high scale of which ran only as high as 40 millivolts. The first break was slightly off scale and was obtained by following the deflection of the null indicating galvanometer. The temperature at which the break occurred was quite definite and was near enough to 40 millivolts to allow a good estimate to be made.

<u>Analysis of data</u>: The curves are shown in Figs. 12 to 20, inclusive. Only one for each alloy is pictured and it will be noticed that beginning with A47, where use of the Brown potentiometer was begun, the abscissae run from right to left. There are two distinct types of curves, each representing distinct processes, and there are a few more, the significance of which is not entirely clear. Alloys 9, 10, 11, 40, 19, and 47 have curves which show the existence of a single phase just below the melting point. There is an initial break, representing the liquidus, and an end-point representing the solidus. The solidus points are probably low for two reasons. In the first place, it is probable that the liquid and solid phases were not in equilibrium during the whole period of solidification. This effect is discussed further in the section on the metallographic work. The second reason is that towards the end of the solidification process, there is a larger temperature difference between sample and surroundings which tends to draw heat out of the sample more rapidly, and there is also a smaller amount of sample left to give out heat. Therefore at end-points of curves, a tailing off is usually noticed. The solidus temperature was selected as the inflection point in this tail and this was quite possibly only a lower limit. The curve for alloy 53, for example, shows this more rapid cooling immediately at the end of the solidification and a subsequent slowing up as soon as the steady-state was restored.

Most other alloys showed not only an initial break but also a second one, plus one or two end-points, showing where precipitation of a species stopped. Occasionally super-cooling occurred; see for example Figs. 15 and 17, A42 and A52. This was usually not a serious problem, and an extrapolation to the liquid cooling curve was easily made.

In order to determine the general form of various types of curves, two alloys each in the binary systems of manganese and of indium with copper were prepared and cooling runs made. The phase diagrams of these systems have been worked out (22) (23) and are shown in Figs. 6 and 7. The cooling curves could therefore be correlated with the actual transformations. Both copper-manganese alloys were homogeneous in the solid phase. Their cooling curves are shown in Fig. 12 (A9 and A10), and the data obtained from them is given in Table III. Reasonably good agreement is noted between the temperatures of thermal arrests and liquidus and solidus temperatures obtained from the diagram. A54 was approximately a eutectic composition in the copper-indium system and its cooling curve is shown in Fig. 18. A29, Fig. 14, showed a peritectic transformation, including the invariant temperature. In these two alloys, the temperatures of thermal arrests were lower than those given in the diagram. The previously reported temperature of the eutectic was 679° C. and that of the peritectic was 715° C. (23) In the present work, values of 661° C. and 705° C. were obtained. Hume-Rothery (32) gives a value of about 710° C. for the peritectic reaction, a value which he obtained by microscopic methods.

Reactions similar to peritectics and eutectics can occur in a ternary system, the difference being that in the ternary system the temperature of three-phase equilibrium is not invariant and the cooling curve will show a second break, but no plateau. If the composition is such that no ternary eutectic is nearby, the curve will next have one or two end-points, depending upon the type of transformation taking place. If a two-phase region exists at lower temperatures, such as does in eutectics and partially in peritectics, only one end-point occurs. If the system goes over to a single solid phase, characteristic of peritectic reactions, a second end-point must occur. Experimentally it was found impossible to determine the number of end-points from the cooling curve, since the tailing-off effect sometimes obscured one. However, the nature of the underlying solid phase could be determined microscopically from the quenched alloy.

Many of the secondary breaks and some of the primary breaks were followed by flat portions of the curve, which sloped off gradually. Since the temperatures of these breaks on various curves did not coincide, it was decided that these were not evidences of ternary eutectics. Instead they were thought to be regions of univariant 3-phase equilibria in which the temperature difference between the beginning and end of the region was comparatively small.

Occasionally smaller breaks were observed below the point at which solidification appeared to have ceased. These were probably solid state transitions and no attempt was made to systematically study them.

Table III contains the temperatures of the thermal effects and in Fig. 8 are shown contours of the liquidus points. A physical model of the composition-temperature diagram was made by drilling holes in a flat board and inserting pegs of such lengths that the top of the peg indicated the liquidus temperature. Other breaks were indicated by rings drawn around the pegs at appropriate heights. The liquidus surface is found to slope downward

TABLE III

Temperatures of Thermal Arrests

(Degrees Centigrade)

	Breaks				End Points		
Alloy	Prim.	Sec.	Tert.	Solid State	#1	#2	Solid State
9	980				928		
10	890				866		
11	870				848		
15	745	735			708		
17	801	783			748		
19	700			599	646		
20	649	625			609		
21	616				565?		
22	600				511		
23	572				509		
24	553				509		
25	547				512		
26	532				501		
27	521				501		
29	719	705			685		
32	865	686			678		
33	826	695			682		
36	797	704			680		
38	752	711			693		
39	663				652		
40	687				656		
41	679			627	642		
42	621				599		
43	650				636		
44	590	510			?		
45	750	729			705		
46	797	692			682		
47	717				660		
48	660	637			619		
49	608				513		
50	578				518		
51	727	710			686		
52	640	619			611		
53	725	700			677		
54	661						
55	617				579?		
56	738	691			670		
57	626	623			612		
58	607				577?		
59	661	652	633		630		
60	626				605		
61	674	656			653		
62	661	647			641		
63	1020*	955*	917*				
64	651				638		
65	636	611			609		
66	705	520			517		

* uncorrected

from the copper corner and no valleys are observed in this surface. When the region of the β-phase is reached, however, the slope becomes much more gradual, as is apparent on reference to the contour map.

The correlation of the cooling curve data will be made in a succeeding section, together with the data of other parts of the research.

Physical Appearance of Alloys: The alloys containing lesser amounts of indium were somewhat soft as prepared, could be crushed only with difficulty or not at all, and were silver colored, sometimes with a slightly yellowish tinge. With increasing indium content, the alloys became quite brittle, especially in the vicinity of atomic composition about 60Cu15Mn25In. Some of the specimens in the region of alloy 55 showed a pinkish color which may have been due to a copper-rich phase present. Alloys with more than about 30 atom % indium were very soft and greyish, and could be easily scratched with the fingernail. With the exception of the binary alloys and alloy 32, all were ferromagnetic to some extent. This was determined qualitatively by the strength of attraction to a small Alnico magnet. The alloys most strongly attracted were those in the vicinity of the atomic composition 50Cu25Mn25In, though little difference was noticed at composition differing by 10 atomic percent.

C. Chemical Analyses

General Discussion: Analyses of the first few alloys showed that manganese and indium were being lost systematically. The losses were attributed to absorption in the crucibles, since they appeared greyish after a run, although some metal may have been lost by evaporation. For this reason, all of the alloys were analyzed to determine their exact composition and also to test the homogeneity of the alloy. Two samples were removed by chipping or drilling from near the top and bottom of each alloy and were analyzed according to the scheme below. In many cases, the two results agreed to .2 or .3% of the total. In many others, differences of up to 1 or 2% of the total were noted. When greater differences were encountered, the specimens was either remelted or a new one prepared.

It must be emphasized here that although in some cases a high degree of homogeneity was not attained, the results are not necessarily invalidated. For in this sort of problem, phase boundaries and other equilibrium lines and surfaces can rarely be located with one or two alloys, but must await the combined results of many preparations. Even then, the locations are approximate. Thus, the contribution of each individual point to the final result, though important, may be only a relatively small part. It was noticed that alloys which were later found to be unacceptable on this basis, gave cooling curves which were practically identical in form with those of the homogeneous alloy.

Procedure: In most cases, only manganese and copper were determined in the specimens. In a few cases, indium was determined, and the results gave 100% total to within several tenths of a percent. The component metals were very pure at the start, and the only impurity which was likely to be introduced was a small amount of oxide from residual air in the system. This was apparently a surface layer and could be removed mechanically or by washing in acid. The indium analysis was therefore omitted and the amount determined by difference.

The separations and determinations are taken from "A System of Chemical Analysis" by Swift (see bibliography) and the procedure is as follows:

A 200 to 800 milligram sample was dissolved in 20 cc. of 16 normal nitric acid, heated to boiling and $KClO_3$ added until the vigorous reaction ceased. The solution was boiled for a few minutes to expel all the ClO_2 and then filtered through an asbestos filter. The precipitate was washed three times with hot water and then redissolved in a solution of 10 cc. of 12 normal HCl and 3 grams of KI in 40 cc. of water. Iodine was liberated according to the reaction

$$MnO_{2(s)} + 3I^- + 4H^+ \longrightarrow 2H_2O + Mn^{++} + I_3^-$$

and was titrated with standard 0.1 normal $Na_2S_2O_3$ solution, using a starch end-point. The filtrate and washings were neutralized with ammonia and made just acid. Three grams of KI were added and the liberated iodine was titrated with 0.1 normal $Na_2S_2O_3$, using starch indicator. 2.5 grams of KSCN were added just before the end-point. The KSCN is said to remove the adsorbed iodine from the precipitate of cuprous iodide, (24) giving a sharper end-point and more accurate results.

In the event that indium was to be determined, the filtrate from the manganese separation was made alkaline with ammonia and digested on a hot plate for an hour. The precipitate of indium hydroxide showed a great tendency to carry down copper, and it was therefore necessary to dissolve and reprecipitate the indium. The precipitate was then filtered through a previously weighed and ignited asbestos filter and heated to about 800° C. to constant weight. The formula of the oxide is In_2O_3. (25)

Another variation of the indium determination was to filter the precipitate of cuprous iodide and precipitate the indium from the filtrate. Apparently some copper was carried down here, judging from the color of the precipitate, though its concentration in the filtrate was very small.

Difficulties in the analyses: A volumetric method for indium was located (26) in which a titration with potassium ferrocyanide was performed, using diphenylbenzidine as an oxidation indicator. This was found to be very satisfactory, due to a fading end-point and an unpronounced color change. The copper titration was very unsatisfactory, and no trouble was experienced. In the case of manganese, it was found that determinations of manganese carried out on the same amounts of pure metal and on reduced standard permanganate (about 50 milligrams) gave results consistently low by about one percent. Use of the Volhard and bismuthate methods (27) resulted in no improvement. Inasmuch as the manganese seldom ran more than 30% by weight of the total, the error would usually be less than 0.3%, and it was decided to accept this accuracy.

The results of the analyses are shown in Table IV. Due to the uncertainty in the manganese determination and inhomogeneities in the alloys, these compositions are probably no more accurate than 0.5% of the total. Those which are known to be less accurate are so designated.

D. Heat Treatment of the Alloys

Brief Description: One of the primary objects of this research was to determine the equilibrium phases just below the solidus temperatures. The alloys as prepared were cooled to room temperature over a period of about two hours, and their structures were presumably different from the high temperature ones. Therefore the alloys were heated at temperatures just below the solidus in order to develop the desired structures, and then quenched in order to preserve them.

TABLE IV

Chemical Analysis of Alloys

	Atomic Percent				Atomic Percent		
Alloy	Copper	Manganese	Indium	Alloy	Copper	Manganese	Indium
4	57.4	21.5	21.1	43	64.0	10.7	25.3
9	84.6	5.4	- -	44	52.0	14.9	33.1
10	68.3	31.7	- -	45	64.1	27.5	8.4
11	65.5	33.1	1.4	46	74.6	17.9	7.5 *
15	65.0	24.9	10.1	47	53.6	32.8	13.6
17	57.1	37.2	5.6	48	50.0	30.0	20.0 *
19	59.0	25.9	15.1 *	49	45.4	28.0	26.0
20	53.9	25.9	20.2	50	44.4	21.0	34.6
21	52.1	24.0	23.9	51	66.9	22.3	10.8
22	47.0	23.7	29.3	52	59.0	19.0	22.0
23	43.0	21.0	36.0	53	70.7	15.8	13.5
24	40.1	19.1	40.8 **	54	73.7	- -	26.3 ‡
25	37.0	17.0	46.0 **	55	53.0	23.6	23.4
26	33.4	15.1	51.5 **	56	75.3	9.6	15.1
27	27.6	12.9	59.5 **	57	55.6	22.8	21.6
29	80.1	- -	19.9	58	50.2	24.2	25.6
32	84.0	5.9	10.1	59	59.0	20.8	20.2
33	77.2	13.4	9.4 *	60	35.6	44.9	19.5
36	73.4	17.8	8.8	61	69.9	9.3	20.8
38	77.5	5.1	17.4	62	62.7	17.2	20.1
39	69.6	5.2	25.2	63	14.3	65.0	20.0 *
40	71.0	12.0	17.0 **	64	63.6	13.7	22.6
41	65.9	18.0	16.1	65	55.6	19.2	25.2
42	57.6	17.2	25.2	66	18.0	32.2	49.8

The following alloys were analyzed for all constituents:

		Weight Percent		
Alloy	Copper	Manganese	Indium	Total
20	47.7	19.5	33.1	100.3
29	68.9	- -	31.6	100.5
64	54.3	10.1	34.8	99.2
9	86.2	13.4	- -	99.6
10	71.4	28.2	- -	99.6

‡ No analysis; composition as weighed out initially

* compositions uncertain by ± 1% due to inhomogeneity

** compositions uncertain by ± 2-3% due to inhomogeneity

Apparatus: The annealing furnace is shown in Fig. 3. A quartz tube surrounded by an electric combustion furnace and insulated for some distance at either end by cans of asbestos comprised the apparatus. The bottom was removable for quenching, and the top, through which the sample and thermocouple were loaded, was closed by a Pyrex disk, waxed on with Apiezon sealing wax W. Connection to the vacuum pump, mercury manometer and argon tank was afforded by the side arm near the top of the quartz tube.

An alundum cylinder which rested on a copper disc supported by chromel wire provided the sample holder. The copper was covered by a layer of powdered magnesia to prevent contact with the sample. The chromel wire was threaded through a porcelain insulator and was supported by a steel rod in the vacuum inlet. Upon removal of the rod, the sample could be quickly dropped into the quenching bath.

Temperature was measured by couple #2, which was led in through two notches in the quartz tube at its top, and which extended down almost to the surface of the sample. The couple was connected to the control circuit of the Brown potentiometer, which controlled the heating circuit of the furnace. In this manner any desired temperature could be maintained. In Fig. 5a is shown a diagram of the heating circuit. The control circuit in the Brown instrument was simply a single pole double throw mercury switch which was activated mechanically by the indicator mechanism whenever the temperature passed through the desired point. With proper initial setting of the Variac and resistor, the temperature could be maintained constant to within one degree centigrade. Due to the semi-open ends, however, a large temperature gradient existed in the furnace. It was determined that over the region occupied by the sample and couple, the variation was less than ten degrees centigrade.

The temperature selected for the annealing was always sufficiently far away from the solidus so that no melting could occur.

Procedure: The sample to be annealed was crushed to granules a millimeter or so in diameter, or else as small as possible, placed in the container, and hung in the furnace. The thermocouple was suspended by its own lead wires from the entrance at the top of the quartz tube. Evacuation of the system was begun and continued for about half an hour, when argon was let in at a pressure of one atmosphere. The course of the temperature-time curve was observed on the Brown indicator only until it was certain that the correct Variac setting had been made.

All alloys were annealed in the furnace at least twenty-four hours. It was thought that since temperatures near the melting point were used, diffusion and rearrangement processes should occur fairly rapidly. To determine whether this period was sufficiently long for equilibrium to occur, two alloys were annealed for varying periods. Samples of A4 were annealed for 24 and 48 hours; A22 were annealed for 24 hours and 6 days; subsequent microscopic examination showed little or no difference in the structure of the samples.

At the end of the period of annealing, the samples were allowed to drop into 600 or 700 cc. of cool distilled water, which was being vigorously stirred. The container always came apart and scattered its contents throughout the quench bath, thus insuring complete and rapid quenching. A film of oxide always appeared on the samples after the quench, and was probably due to the reaction with water. The coating was removed by washing in dilute hydrochloric acid, rinsing in distilled water and acetone, and allowing the sample to dry.

E. Metallographic Studies

Preparation of Specimens: Before an actual examination of a specimen could be made, it had to be properly mounted and prepared. The alloys were mounted in transparent lucite discs half an inch thick and one inch in diameter. Lucite powder, specimen, and label, were placed in a steel cylinder, heated to 150° C., compressed to 3500 pounds per square inch, and chilled with tap water. The lucite pellet could then be forced out of the cylinder and ground down to the surface of the metal on an emery wheel. Further grinding was done successively on 280, 320, and 400 grades of Aloxite paper, which was kept wet during the operation. The specimen was thoroughly rinsed between two successive operations to prevent larger grit particles from being mixed with the next smaller size. Rotation of the direction of motion by 90° on each successive paper provided a method of determining when sufficient grinding had been done, since then the scratches from the preceding paper were removed.

Further polishing was done on two motor-driven wax wheels, using suspensions of #500 and #600 emery powder in liquid soap as the abrasive. Progress of these polishing operations was observed under a microscope using a magnification of 75 times. Usually sufficient polishing could be accomplished on the #600 emery wheel, leaving only a few scratches of any size on the specimen. In many cases, however, final polishing was done on a cloth covered wheel, using levigated alumina and distilled water.

The metallic surface now appeared smooth but uniform, although occasionally a structure was faintly visible at this point. To develop the structure the alloy was etched, usually in either 10% ammonium persulfate or in a solution containing potassium dichromate, sodium chloride, and sulfuric acid in distilled water. Other solutions were used, such as ferric chloride in dilute hydrochloric acid, ammoniacal copper ammonium chloride, nitric acid, and ammoniacal hydrogen peroxide, but the first two seemed to give the best results. The procedure was to immerse the specimen in the solution; for persulfate, an immersion time of 30 seconds to two minutes usually sufficed, and for the dichromate, 5 to 10 seconds.

The shading and contrast caused by both dichromate and persulfate were about the same. In cases where the dichromate attacked the metal, a fine structure was visible at magnifications of 1000 times, but these were not visible using persulfate, and may have been due to uneven attack by the reagent. See for example Figs. 23 and 24, A43 and A52. Persulfate, however, had the advantage of giving contrast in homogeneous appearing alloys; that is, differently oriented grains of a single phase were attacked at different rates, giving a good contrast and permitting grain boundaries to be observed. See, for example Fig. 24, A56.

Examination of Specimens: Examination of the etched surface could now be made, either visually or photographically. Photomicrographs of most of the quenched alloys were made, in addition to some of the unannealed ones. Only a few photographs were taken of homogeneous alloys for illustrative purposes, since all were quite similar in appearance. The photographs were taken in a Bausch and Lomb Metallograph, using a green "B" filter and commercial ortho film. Printing was done on Kodak velox paper. A magnification of 75 times was found to be most satisfactory, and was used in most photographs, though both higher and lower magnifications were used.

Analysis of data: Photographs of the alloys are shown in Figs. 21 to 26, inclusive. Their significance in relation to the phase equilibria will be discussed later, but some of the salient characteristics of the structures should be pointed out at this time.

Single phase structures were recognized through one of two features: either there was an even etching over the whole surface of the alloy, or else contrast was observed, but the grains were large and the boundaries were more or less straight lines. In the latter case no overall pattern in the specimen was observed; that is, any one grain did not appear to bear any relationship to any other grain. Examples of this type of structure are shown in Fig. 24, A51 and A56. A41 showed this type of structure, though the grain size was much smaller than that of any other sample.

All other alloys appeared to contain just two phases, although in some cases, three may have been present. The chief identifying mark in the two phase alloys was the appearance of a dendrite or "Christmas tree" structure. This is caused by growth of the primary crystal in a particular direction and subsequent growth of "side-arms" or "branches" on the main crystal. Examples are shown in Figs. 22 and 26, A33 and A4. This probably indicates a non-equilibrium condition during the solidification process. Since the solid phase should change composition during solidification, it would be expected that the crystals would redissolve and others of different composition would precipitate. This does not seem to have occurred in these cases, and unless diffusion was very rapid, the dendrite probably has a variable composition. However, in the annealed alloys, these forms were not often visible, although the remnants of them could be seen. For example in Fig. 23, A45, a regular arrangement of the light areas is noticed, indicating the position where a dendrite existed, and had been broken up on annealing. This feature usually made it possible to distinguish the primary crystal from the matrix, or from whatever the secondary precipitation product was.

One other type of structure was observed. Alloys 22 and 50 contained many cracks and holes after final polishing, and etching had little effect on the structures. The alloys were fairly soft to begin with, although the cracks were probably the sites of a much softer phase which was removed during polishing.

Determination of the appropriate location of phase boundaries was aided in the case of two-phase alloys be estimating relative percentages of the two areas in a photograph. This ratio should give the relative distances of the alloy composition from nearby phase boundaries.

Curie Point Studies

Apparatus: Curie points were determined in the apparatus shown in Fig. 4. This method is essentially the same one used by Ewing (43) in his early researches on magnetism. The furnace consisted of a copper tube one inch in diameter and 24 inches long, on which resistance wire was wound from one end to the other and then back upon itself. This winding produced no resultant magnetic field. Asbestos lagging served as insulation for the tube and winding. The furnace was 32 inches long and had a small opening in one end to admit a thermocouple and was completely open at the other end to admit the sample. An asbestos plug was used to seal up this end while the furnace was in use.

A magnetizing solenoid, four feet long and six inches in diameter, with four layers of #18 cotton covered wire, provided the magnetizing field. A balancing coil, 12 inches long and 1½ inches in diameter provided a field to counteract the solenoid field at the magnetometer. The magnetometer was merely an instrument containing a small bar magnet 2 cm. x 4 mm. x 1 mm., suspended on a ten inch fiber in the horizontal plane of both coils. On the suspension were attached also an aluminum vane for air damping, and a small mirror. The whole suspension system was enclosed to prevent interference by air currents and a window was provided in front of the mirror. At a distance of six feet from the magnetometer was a lamp and scale. The light was focused by a condensing lens in front of the bulb and reflected by the magnetometer mirror back to the scale.

Samples in the form of Pyrex tubes filled with crushed or powdered alloys were used. These were usually six to eight millimeters in diameter and about 20 centimeters long. By experiment it was determined that the variation in temperature of the inside of the furnace over this length was about 2° C. at the highest temperatures employed. A calculation of the magnetic field showed that it was constant to better than 0.1% over this same region.

The solenoid and balancing coil were placed on an east-west line. The coils were parallel and their respective distances from the magnetometer adjusted so that with no sample in the large coil and the D. C. magnetizing current on, no deflection of the light beam was observed. Fig. 5b shows the circuit diagram of this apparatus. Since the magnetic field due to the sample measured at a point on its transverse axis is parallel to the longitudinal axis of the sample, the magnetometer is acted upon by two fields at right angles to one another. The earth's field, though subject to a diurnal variation, could be considered essentially constant over a period of an hour, which was about the length of time needed to run an experiment. Therefore the deflection of the light beam was a measure of the intensity of magnetism of the sample.

Some trouble was encountered with stray external fields and pieces of nearby iron. All movable iron was removed as far as possible,from the apparatus and all other iron, such as doors and other equipment, was not touched during an experiment. In spite of these precautions, the light beam occasionally oscillated over a range of several millimeters. However, since many points were taken during a run, and since the total deflection of a magnetized specimen was usually 10 or 20 centimeters or more, this difficulty did not seriously hinder the work.

Couple #3 was used in this work and was enclosed in a 6 mm. Pyrex tube and inserted into the furnace, so that the hot junction was close to the center of the sample. A cold junction was used and the emf read on a Leeds and Northrup Student Potentiometer. The couple was calibrated at only one point; namely, the freezing point of U. S. Bureau of Standards lead. A resistance furnace was used to heat the lead. The Pyrex tube containing the couple was immersed in the molten lead which was contained in a graphite crucible and covered with powdered graphite. Emf readings were taken on the type K potentiometer and plotted to obtain the freezing curve.

Procedure: In making a run, the coils were properly adjusted to balance each other and a reading of the light beam made. The sample was put in the furnace and heating begun. Usually a heating rate of about 5° C. per minute was used. The D. C. magnetizing current was adjusted to 2.10 amperes before each reading so that the magnetic field would be constant. This current produced a field of 82 gauss inside the solenoid. Simultaneous readings of thermocouple emf and light beam deflection were recorded until the Curie point was reached. The sample was removed, a null reading taken, and the sample returned to the furnace. A set of readings was then taken while the specimen cooled at about the same rate (5° C. per minute).

In the case of alloys which gave no deflection, the pyrex tube containing the alloy was dipped in liquid air for 5 to 10 minutes, andreplaced in the furnace. On several occasions this treatment produced a deflection which soon disappeared, showing that the sample possessed a Curie point below room temperature. No attempt was made to measure these temperatures.

Measurements were made of Curie points of the alloys as prepared and cooled in the furnace and also after quenching. A third set of measurements was made on the quenched alloys after they had been heated for 200 to 300 hours at 100° C. In Table V are recorded these results, together with the heat treatments used. The reasons for this treatment will be discussed later.

Analysis of data: In general, the forms of the plots of light beam deflection versus temperature were similar to those in Fig. 27. From such a curve, the ferromagnetic Curie point Θ_f (28) is determined by extrapolation from the point of maximum slope to the temperature axis. This method of obtaining Θ_f involves a slight error, for the following reason. According to the Weiss theory of ferromagnetism, (29) (41) the curve of temperature versus intrinsic magnetism, or intensity of magnetization in the absence of an external field, should cut the temperature axis at a definite angle. This temperature should coincide with the paramagnetic Curie point, which is determined from susceptibility temperature measurement at higher temperatures. The Weiss theory predicts that at sufficiently high temperature, all substances become paramagnetic and obey a law of the form

$$\chi = \frac{C}{T-\Theta}$$

where χ is the susceptibility per mole, T is the absolute temperature, and C and Θ are constants and depend on the substance under consideration. Furthermore, at the temperature $T = \Theta$, where the denominator in the above expression vanishes, the substance becomes ferromagnetic. By means of experimental determination of χ as a function of T at higher temperatures the value of Θ may be determined and is known as the paramagnetic curie temperature. A third phenomenon which is predicted to occur at this temperature is a peak in the specific heat curve. Actually a tailing off of the magnetization-temperature curve is

TABLE V

Curie Temperatures and Heat Treatments

Alloy	Curie Temp. Unannealed	Initial Annealing		Curie Temp. Freshly Quenched		Reannealing	Curie Temp. Reannealed	
		Temp. °C.	Time Hours	Rising Temp.	Falling Temp.	Time at 100° C.	Rising Temp.	Falling Temp.
4		530	24					
11	279							
15	269	693	24	None		380	< R.T.	
17	277	704	24	< R.T.		150	144	
19	246	628	24	135	139	290	151	142
20	208	582	24	181	177	290	198	179
21	265	556	24	261	259	290	262**	259
22	276	505	6 days	255		240	272	264
23	280							
24	223 & 268							
33	228	653	29	> R.T.		250	> R.T.	
36	244	653	24	R.T.		170	R.T.	
38	*	679	24	None		360	< R.T.	
39	206	633	46	None		260	None	
40	203	633	24	None		330	< R.T.	
41	224 & 135	592	40	205	200	350	212	203
42	270	582	35	< R.T.		260	< R.T.	
43	#	612	43	None		200	None	
44	280							
45	279	670	24	None		330	115	
47	244	653	25	171	159	290	177	160
48	261			233		330	232	
49	294	507	22	285	281	340	288	
50		507	22	258	268	340	272	
51	269	673	27	< R.T.		250	117	
52	79 & 225	587	24	169	181	336	203	183
53	234	663	25	< R.T.		350	101	
55	266	566	30	244	243	260	260	249
56	190	653	24	None		250	750	
57	230	602	24	198	198	260	210	203
58	268	561	63	253	254	200	264	263
59	90 & 227	602	26	172	167	260	183	167
60	286							
61	66 & 202	633	24	None		250	< R.T.	
62	110 & 212	633	24	R.T.		240	122	
63	293							
64	65	612	24	None		220	None	
65	265	592	24	132	125	190	247	239
66	283							

* Alloy was magnetic, but too weak to give sufficient indication in Curie apparatus

** After further annealing at 350° C. for 3 days, this alloy had a Curie point at 266° C.

\# Alloy was magnetic, but insufficient sample prevented Curie point determination

R.T. stands for Room Temperature

observed and the paramagnetic Curie point, Θ_f, is usually found at a temperature 15° - 20° C. higher than Θ_f. (28) The specific heat anomaly appears at the temperature of maximum slope of the curve. In the absence of an external field, the determination of Θ_f temperature appearing in the Weiss theory gives a value slightly lower than the temperature determined in the presence of an external field. (30) Stoner (30) gives an approximation for the difference caused by a field. In the case of the relatively weak fields of about 80 gauss used here, the difference would be about 2° for iron and 1° for nickel. The magnitude of the correction for these alloys is not known, but is presumably of the same order of magnitude, and is therefore neglected.

The Curie point curves took various forms, as shown in Fig. 27. These include a temperature hysteresis, varying size of tails, and double Curie points, and will be discussed in the following section.

Discussion of Results

A. Phase Equilibria

As a preliminary note, it should be stated that the designations of the various phases are those used in the description of the corresponding phases in the binary copper-indium system, which have been applied by previous workers. The α-phase has the cubic-closest-packing structure of pure copper, while the β-phase has a body-centered cubic structure. (32) Although the binary β-phase does not occur quite at an electron: atom ratio of 3:2, Hume-Rothery considers it a β -type phase, (32) displaced slightly from its predicted position due to the influence of the large size of the indium atoms. The binary γ-phase is not obtainable by quenching, though its low-temperature form (δ) has the γ-brass structure typical of the Hume-Rothery γ-phases. (46) As for the designation β', this is the conventional one for β-structures which are ordered.

$\alpha/\alpha+\beta$ and $\beta/\alpha+\beta$ boundaries: The copper-indium (23) and copper-manganese (22) binary phase diagrams are shown in Figs. 6 and 7. It will be noted that in the copper-rich portion of the copper-manganese system, a continuous solid solution exists in the region of the solidus. In the copper-indium system, however, several phases occur, and the α-and β-phases are related by a peritectic transformation. As discussed earlier, such a reaction will exhibit on its cooling curve an initial break corresponding to crystallization of the α crystal, and a plateau at the peritectic temperature. If the composition is such that the solid phase will be a mixture of α and β crystals, then the cooling curve will show just the end-point of the plateau. If the overall composition is such that the solid phase is pure β, then a second end-point will occur at the temperature at which the reaction liquid $\rightarrow\beta$ is complete. It has been already pointed out that when such a transformation is extended into a ternary system, the peritectic reaction no longer occurs at a constant temperature, due to the extra degree of freedom possessed by the ternary system. That this type of transformation occurs in this system can be recognized from a combination of thermal and microscopic data.

Alloys 9, 10, and 11 all show the same type of cooling curve. This is the familiar one of a break and end-point, characteristic of the crossing of solidus and liquidus lines above a homogeneous phase. By inspection of the cooling curves it may be seen that Alloys 15, 17, 45, 51, 36, 46, 33, 53, 32, 56, and 38 show two breaks and at least one end-point. Reference to the composition key in Fig. 9 will also show that these constitute the copper-rich alloys of this investigation. It was not possible to determine by inspection whether one or two end-points appeared on most of these curves, probably because the tailing off effect obscured the first one. The structure of the underlying solid phases was obtained, however, from the metallographic work. Alloys 32, 33, 36, 45, and 17 consisted of two phases, while 29, 38, 56, 53, and 51 were homogeneous. The homogeneous alloys appeared essentially identical under the microscope, and only photographs of alloys 51 and 56 were taken. The α-phase shows up as the lighter color in the two-phase alloys, and by estimating the relative amount of the two areas, an approximate location of the high temperature phase boundaries was made. These boundaries are shown in Fig. 9 as broken lines. It should be emphasized that these lines do not represent an isothermal section, but are the projection on an isothermal plane of the boundaries at the solidus temperatures.

The solid line starting at the copper-indium binary side at 21 percent indium represents the extension of point A in the binary diagram. The location of this line is obtained by an observation of the secondary breaks in the cooling curves, and is the locus of the liquid composition at the temperature where the reaction α + liquid $\rightarrow \beta$ begins. It will be noticed that in the sequence of alloys 17, 45, 15, 51, 53, 56, 38, and 29, these temperatures drop to a minimum and rise again, reaching a maximum at 38, then dropping again at 29. Alloys 32, 33, 36, and 46 have their secondary break in the vicinity of the minimum. The type of equilibrium existing in the neighborhood of A15 is illustrated in Fig. 10a, where an isothermal section corresponding to about 730° C. is shown, and in Fig. 10b, where a vertical section corresponding to about 20 atom percent manganese is shown.

As we consider alloys with composition approaching the minimum mentioned above, the size of the three phase triangle in Fig. 10 becomes smaller and a situation analagous to a binary minimum melting point results, such as appears in the copper-manganese system. At the minimum, the points E and C will fall on the lines AB and DF respectively, and the system will be invariant. On the other side of the minimum, the three phase triangle will again appear, but in Fig. 10a, the point C and the β region will be below AB. The presence of the maximum at A38 is uncertain, since only one alloy was prepared in this region. While the curve could conceivably have both a minimum and a maximum, a discrepancy might arise due to uncertainty in the temperature measurement.

It should be pointed out here that the microscopic and thermal data do not entirely supplement each other. The thermal data gives information at the temperatures of solidification, while the microscopic data obtained is at the annealing temperature, some ten or twenty degrees lower. However, this temperature interval is relatively small and should make little difference in the approximate location of the phase boundaries.

β-phase region: The next set of alloys are the homogeneous ones 47, 19, 41, 62, 64, and 40. 47, 19, 40, and 64 showed typical single-phase cooling curves and were homogeneous under the microscope, showing that at these compositions the β-phase is stable up to the melting point. Alloys 41 and 62 were homogeneous when quenched, though the grain size of A41 was much smaller than that of other samples. However, a glance at the cooling curves of these two alloys shows the presence of more than one break. The compositions of these alloys are relatively far away from the peritectic region and the temperatures appear to be too low to have any connection with it. In the event a second peritectic region was present on the indium-rich side of these alloys, this behavior might be observed. As a result, two possibilities arise. The first is that a two-phase region exists roughly along the dotted line in Fig. 9. This line would divide the proposed β-region into two parts, and would account for the breaks in the cooling curves of alloys 41 and 62. A minimum exists in the peritectic line between the α- and β-phases in Fig. 8 (broken line), so that another peritectic line might run from this minimum towards the compositions of alloys 41 and 62. There is some other substantiating evidence for this to be found in the magnetic data. There is also, however, some opposing evidence, the first of which is that there is a continuous string of homogeneous alloys along the copper-rich side of the β-phase. In the event that a two-phase region existed along the dotted line, it would necessitate having a break in this string, although a narrow region of inhomogeneity might have escaped detection. It will be noticed that the microphotographs of homogeneous alloys and others in the $\alpha + \beta$ region which contain areas of β-phase are quite similar in appearance on both sides of the dotted line. This would probably not be the case if the two regions were different types of phases. For this reason a second hypothesis is proposed. This is that the β region exists as shown by the broken lines in Fig. 9 and that the second and succeeding thermal arrests exhibited by alloys 41 and 62 are due to some sort of second-order transition, possibly an order-disorder type, in this region. The dotted line in Fig. 9 is the proposed approximate location of this transition, and is drawn principally on the basis of the magnetic data.

The cooling curve of A41 may then be interpreted as containing the liquidus and solidus points of a homogeneous phase, followed by two more breaks, which are presumably those due to the proposed transition. In A62 the occurrence of the transition is coincident with solidification. There may or may not be a latent heat associated with this transition. In the case of a true second order type, there is only a specific heat anomaly, but even this would probably show up on the cooling curves as some sort of thermal effect. Additional material bearing on this point will be presented in the appropriate sections to follow.

$\beta/\beta+\gamma$ boundary: Nearly all the other alloys showed two phase structure. The binary copper-indium eutectic at 25.8% copper presumably extends for some distance into the ternary system. A54 is of the approximate binary eutectic composition, and photographs of it in the as-prepared condition are shown in Fig. 26. By inspection of the photographs of Alloys 39 and 61 and a consideration of their compositions, it appears that the β-phase shows up as the dark area in this region. A43 contains about a 50-50 division of light and dark areas, and its cooling curve shows only one break, followed by a flat portion. This indicates that this alloy was of the eutectic composition and therefore that the eutectic line must run close by on the copper-rich side or else through this composition. A39 shows the same type of curve but considerably more of the lighter area in the annealed condition. A close examination of the original cooling curve indicates that a second break, more in the nature of a jog, may be present near the end of the solidification. Apparently A39 is close to the $\gamma/\beta+\gamma$ boundary. This boundary was not drawn farther since it is at the edge of the area studied here, and a determination of the remainder of this boundary must await further work in this region.

$\beta/\beta+\beta'$ boundary: The remainder of the alloys are nearly all two-phase ones. A20 and A48 have cooling curves containing two breaks, but A48 is homogeneous as quenched. It appears, therefore, that a second peritectic reaction occurs in this region and the broken line in Fig. 9 indicates the boundary here. Both thermal and microscopic results indicate that alloys 57, 59, 52, 42, 4 and 65 are two-phase alloys. Photographs of A42 are not shown, but its appearance was identical to that of A52. A third break appears on the curve of A59 and may be due to the same sort of thing occurring in alloys 41 and 62. Since the photographs of alloys 59, 52 and 42 contain very little light area, the boundary between the β-phase and this second two-phase region (see Fig. 9) must run close to these compositions and in the indicated direction. It is difficult to see where another phase boundary, such as might run along the dotted line, would connect to this region.

Alloys 21, 55 and 58 have cooling curves with identical forms, the initial breaks occurring within 5 degrees C. of each other. Reference to the microphotographs shows that A55 is definitely a two-phase alloy. A21 contains little or no second phase, while A58 contains a small but definite amount of a second phase. The shape of the cooling curves of these alloys is difficult to explain. Since A21 is nearly homogeneous, its curve could be merely a simple solid solution type. However, with the data available, it is impossible to ascertain the nature of the equilibria present in this region of the composition diagram. One further point should be mentioned, however. Hume-Rothery and his co-workers (11) have prepared an alloy of the composition Cu:Mn:In equal to 51.5:24.5:24.0, and have found it to be homogeneous and to have the crystal structure shown in Fig. 11a. This superlattice is the same one which is present in the other Heusler-type alloys, and the composition is just on the copper-poor side of A21, an alloy which is nearly homogeneous. It may be, therefore, that a narrow single-phase region exists in the region between A21 and A58, and may extend in other directions. This bit of evidence favors the second alternative for the β-phase boundaries. The superlattice of Fig. 11a exists in the region near Cu_2MnIn, and the region near the binary copper-indium system is an extension of the binary β-phase, both of these having body-centered cubic structures. It would be somewhat surprising to find the intervening phase, namely the area containing A19, to have a different type of structure. Since the one two-phase region containing alloys 57, 59 and 4 is apparent from the photographs, the dismissal of the dotted line as a true phase boundary is called for. This means that this transition must be due to some sort of second order effect, such as a specific heat anomaly or a new type of ordering.

Indium-rich Alloys: Cooling curves for alloys 22, 23, 24, 50 and 49 were all of a similar appearance, as can be seen by reference to Figs. 13 and 17. The end points were all at about the same temperature, but the primary breaks decreased with increasing indium content. Three other alloys, 25, 26, and 27, were prepared, but due to inhomogeneity they are not to be relied upon for meaningful results. The overall compositions of top and bottom of these alloys varied by 3-6 percent; however the cooling curves shown in Figs. 13 and 14 were reasonably clear-cut and the difficulty may be due to segregation during cooling.

The microphotographs of alloys 49, 50, and 22 have been described. The region is one of two phases; one of these is soft, probably rich in indium, and is easily ground away. It may be a liquid phase at the quenching temperature. This last possibility is strongly indicated by an inspection of the copper-indium binary diagram, where the region from 40 atom percent indium on consists at higher temperatures of a solid phase in equilibria with a liquid. Alloy 58 may belong in this group. The photograph shows the presence of a few holes such as exist in A49, though the thermal arrest in the vicinity of 510°C. was either absent or a very small one.

Alloys 60, 63, 66, and 44 were prepared principally as guideposts for for future work. A44 shows a break in its cooling curve at 510°C., the same temperature as the end-points in the nearby soft alloys. A44, however, was brittle like those in the vicinity of A42. Alloy 66 was very soft, and resembled A22 through A28, while A60 and A63 were similar to alloys in the region of A20 and A21.

B. Magnetic Results

Miscellaneous Phenomena: In using the results of the Curie point runs, the most important item is the actual Curie temperature, Θ_f. Some of the other features of these curves are interesting and will be briefly mentioned.

The size of the tail on the curve varies somewhat, though no correlation with composition was noticed. Néel (31) has discussed this "tail" effect and considers it to be due to variation in "domain"size. Weiss' theory predicts that below the Curie temperature a substance will be spontaneously magnetized, a phenomenon which is not observed experimentally. To circumvent this difficulty the existence of "domains", or small regions completely magnetized but randomly oriented, was postulated, so that in the absence of an external field no resultant magnetism is predicted. A review of Néel's work has been given by Bates (44).

The existence of two Curie points in some unannealed alloys is explainable as due to the presence of two separate magnetic phases. More will be said about these alloys.

A temperature hysteresis effect is also present but the cause of it is not certain. Usually the temperature abtained in cooling the specimen was lower than that obtained in heating. In A52, freshly quenched, the reverse was noticed, but on reannealing the normal order reappeared. As a matter of consistency, the recorded Curie points were always obtained from the heating curves.

In some cases, such as Fig. 27, A47, a slight increase in deflection was noticed just before the Curie point was reached. This may be due to the onset of ordering in the alloy at these temperatures.

Previous work: It is generally believed that magnetism in Heusler-type alloys is due to the presence of order in the crystal lattice of the β-phase. The Cu-Mn-Al alloys have been extensively investigated, and an ordered phase has been shown to be present in the magnetic specimens (3) (6) (7). This ordered structure or superlattice is shown in Fig. 11a. The same result was obtained in the Cu-Mn-Sn system by Carapella and Hultgren (8). Fig. 11b showas their results on the limits of the β-phase at high temperatures. Ordering was observed in part of the β region by means of x-ray determinations, and is indicated in the figure.

It has been shown that this same structure is present in the Cu-Mn-In system (10) (11) in the region of the composition Cu:Mn:In = 2:1:1. The composition studied by Hume-Rothery was given in the preceding section. The results of this present research indicate that this structure, or at least some sort of ordered crystal, appear over a much wider range of composition.

In theory no very clear relation seems to exist between Curie point and order or between Curie point and magnetization at saturation. The latter gives a value of the elementary magnetic moment responsible for the magnetism and is of direct interest. However, since the magnetic alloys of this type are always ordered, and especially since by themselves none of the three metals is magnetic, one may assume that some sort of interaction is necessary in the alloy, in order for magnetism to occur. In a disordered crystal, no one atom bears any particular relationship to any other, and consequently little regular interaction will occur. In an ordered crystal, however, any interaction between two kinds of atoms is repeated, so that if any tendency toward magnetism should exist it will be stronger when the crystal is ordered. It appears that the height of the Curie temperature may be considered, qualitatively at least, to be an indication of how much thermal energy is needed to destroy this interaction and therefore to be also an indication of how much order exists in the specimen. If this is the case, higher Curie temperatures will indicate more highly ordered alloys.

It should be pointed out that the specimen with the highest Curie temperatures were found, qualitatively speaking, to be the most strongly magnetic.

Evidence of Local and Long-Range Order: In Figs. 28 and 29 are shown contours of the Curie points as determined on the freshly-quenched alloys and on the same alloys after annealing at 100°C. The highest Curie points are in the region of the Cu_2MnIn composition and do not change greatly during the treatment at 100°C. However, the alloys containing larger amounts of copper showed large increases in their Curie points, suggesting that some ordering occurred. Both contour maps also show that the highest Curie points are roughly on the line of equal manganese and indium concentration. It will be noticed that a sharp drop in Curie temperatures occurs on the indium-rich side of the dotted transition line, while on the opposite side little or no decrease occurs in the Curie temperature.

A distinction should be made here between long range order, which implies the formation of a superlattice like that of Fig. 11a which comprises the whole alloy, and short range or local order, in which a copper atom will have a greater probability of having manganese and indium atoms as neighbors than the atomic proportions would indicate, but no regularly ordered structure is present. Long range order is usually present only in a restricted range of composition, since fairly definite ratios of atoms are necessary, while local order is possible over a much wider range.

Now, the β -phase in the copper-indium system has been shown to have an unordered body-centered cubic type of lattice (32). The proposed homogeneous β region in this ternary system may be therefore assumed to have the same structure. Since the superlattice is known to exist in the neighborhood of Cu_2MnIn, the intermediate two-phase region must consist of this superlattice, which we shall designate β', in equilibrium with the unordered alloy β. This type of situation has been known to exist, for example, in the copper-beryllium alloys (33), so there is some precedent for it. It might be supposed at first that two such similar structures would not show up as two distinct phases, but some other results tend to confirm this hypothesis. In the first place, inspection of the β-phase area in Fig. 9 shows an indentation due to the $\beta + \beta'$ region at the equi-MnIn composition. This may mean that along the Cu_xMnIn line the presence of equal numbers of Mn and In atoms makes the superlattice slightly more stable and the unordered β slightly less so. This situation also seems to fit the facts regarding the effects of annealing at 100° C. In general the alloys in which the β' structure is stable up to the melting point, and in which, consequently, fairly complete order already exists, did not show much increase of curie point on annealing. Those outside this region, however, showed large increases. This effect is attributable to local ordering effects, although it is possible that a low-temperature transition producing β' might occur rapidly enough at 100° C. to produce some effect. This local ordering effect was much more pronounced on the manganese side of the dotted line in the contour maps. The location of the line was made such that those alloys which showed large Curie point increases on reannealing would be above the line. As to the exact nature of this proposed transition, nothing much can be said. However, some general remarks may apply. The alloy 41 and also the dotted line fall nearly along the line of equal manganese and indium content. This may merely mean that beyond this point the manganese atoms get too far apart for interaction and resulting magnetism. It could also mean that a ratio of at least one-to-one of manganese and indium atoms was necessary for the occurrence of magnetism. It is worth repeating that in the Cu-Mn-Sn system the β-phase was found to be ordered (see Fig. 11b), the division between ordered and unordered regions being similar to that proposed here. However, that situation was somewhat different, in that the β-phase contained both the point Cu_2MnSn and the superlattice of Fig. 11a, while in this Cu-Mn-In system the β-phase does not contain the Cu_2MnIn composition and presumably, therefore, not the superlattice.

In the copper-indium binary system, the β-phase is seen to be stable only above 574° C., thereafter decomposing eutectoidally into α and δ. It might be expected that the β-phase will exhibit a similar decomposition in the ternary system. Some evidence for this exists in the contour map of Curie points of the unannealed alloys, shown in Fig. 30. These alloys were cooled to room temperature over a period of about two hours. Here again the Curie points of alloys in the region of Cu_2MnIn are about the same as those of the quenched alloys, indicating that the β' structure may be stable down to room temperature. Two Curie temperatures are exhibited by alloys 41, 61, 62, 52, and 59. Presumably this is a result of partial decomposition of the β-phase into β', the β showing the lower temperature. The striking thing here, however, is the fact that all of the alloys have much higher Curie temperatures than the quenched specimens. This fact was discovered also by Valentiner, who prepared some indium-poor alloys on the composition section joining pure In with the composition Cu_2Mn, and the result was ascribed by him to the existence of the superlattice at these compositions. The additional data obtained here would seem to support the conclusion. It will be noticed that alloys 11, 17, 45, 51 and 15 have Curie temperatures of roughly the same magnitude as the alloys in the region of alloys 21, 55 and 58. Also, the microphotograph of A15 in the unannealed state shows definitely that the alloy is not homogeneous. Probably the β-phase decomposes at lower temperatures to α and β'. This does not entirely explain the situation, since alloys 47 and 17 have Curie points lower than alloys on either side. It may be that these two specimens have compositions near the center of a eutectoid trough, and decomposition might be very slow or might not occur at the low eutectoid temperature. Perhaps sufficient local ordering of the unstable β-phase may then occur on slow cooling to give the high value of the Curie point.

C. Further Remarks

The results of this research appear to be most valuable when considered as a preliminary study of this system, both for the purpose of gaining a general picture of the existing relations, and for the purpose of directing future studies upon the system. One study proposed is the determination of saturation magnetization values from which the moment of the elementary magnetic group or particle can be obtained and also the correlation with the Curie points. Another study is an x-ray determination of the structures of the alloys to confirm the presence of β and β' phases and to determine the exact structures in the region studied. Further detailed phase equilibria work is needed in the vicinity of the composition Cu_2MnIn to determine exactly the extent of the β' phase. A further interesting point is found in the fact that the manganese-indium system has been suggested to be ferromagnetic (34). In view of this and the fact that alloys 60, 63, and 66 are ferromagnetic, it would be expected that other phases or compounds in this Cu-Mn-In ternary system are also magnetic.

PART II.

Introduction.

During the course of the chemical analyses which were performed during the work on the copper-manganese-indium alloys, it was found that no reliable volumetric method for the determination of indium was known. One volumetric method was found, but it gave poor results (26). A gravimetric method is known (25), but was tedious and time-consuming, and partly for this reason, the determination of indium was omitted from the analyses of these alloys. It was decided to explore the literature of the chemistry of indium to see whether some of its reactions and properties would be suitable as a basis for a volumetric method of determination. Three possibilities were uncovered, one of which gave promise of being quite satisfactory, and due to time limitations, somewhat incomplete. The data, however, might form the basis of a further attack on the problem.

Previously Reported Methods: The earliest method known for the determination of indium was the gravimetric one previously referred to. A volumetric method has been reported (26,35) based on the titration of indium with ferrocyanide. Indium forms an insoluble compound with ferrocyanide, the formula of which is $In_5K[Fe(CN)_6]_4$. (36). Thus at the end-point an oxidation-reduction indicator may be used, provided some ferricyanide was originally present to oxidize the indicator. According to both references, the titration must be done in 60% or stronger acetic acid. Sample results, using the method, were given by Hope, Ross and Skelly (26), but only to about one percent. Attempts to use the method in the alloy analyses showed the method to be unsatisfactory, since the end-point faded rapidly and the color change was not sharp.

A potentiometric method was devised by Bray and Kirchmann (36), in which results accurate to .1-.2% were claimed. Potassium ferrocyanide was the titrating agent and titrating solutions of very low ionic strength were necessary in order to get a sharp voltage drop at the end-point.

Experiments on Indium Iodate and Oxalate

Indium Iodate: The solubility of indium iodate, $In(IO_3)_3$, in water has been determined by Ensslin and Dreyer (37) and is 0.53 grams per liter in a neutral solution at 20°C. The solubility increases quite rapidly if nitric acid is added to the solution. Using this figure for the solubility, the solubility product is calculated to be 1.3×10^{-11}, and if the concentration of the iodate were made, say 0.1 formal, the concentration of indium in the solution, providing no complexing occurs, is calculated to be 1.5×10^{-3} milligrams per liter. In 0.2 formal nitric acid solutions, the solubility is given as 1.3 grams per liter and the corresponding indium concentration in 0.1 formal iodate is 2.6×10^{-3} milligrams per liter.

It would appear that by adding an excess of a soluble iodate to a neutral or weakly acid indium solution, quantitative precipitation of indium should occur, and furthermore that the precipitate might be redissolved and titrated iodometrically.

A series of experiments were performed to determine whether the indium could be precipitated quantitatively and whether the precipitate was of constant composition.

0.5 formal solutions of KIO_3 and $NaIO_3$ were prepared by dissolving the Bakers C. P. reagents in distilled water. Two indium solutions, approximately 0.1 formal, were prepared by dissolving weighed amounts of 99.97% pure indium metal in slight excess of nitric acid and diluting to 250 cc.

The nitric acid concentrations were 0.4 formal and 0.1 formal respectively in solutions No. 1 and No. 2. 10 cc. of indium solution were pipetted out for each experiment, and a known excess of iodate added. The precipitate was filtered, washed with cold water, redissolved in a solution containing 5 cc. of 6 normal H_2SO_4 and 3 grams of KI in 35 cc. of H_2O. Titrations were made with a 0.5 normal solution of $Na_2S_2O_3$, previously standardized against potassium dichromate. Completeness of precipitation was tested for by making the filtrate alkaline with ammonia. Absence of cloudiness was taken to indicate complete removal of the indium. The results are shown in Table VI.

It was thought that alcohol might decrease the solubility of the indium iodate, and in experiments 10 and 11 5 cc. and 4 cc. respectively of denatured alcohol were added to the solution before the addition of the indium, no precipitate occurring until the indium was added.

In experiments 1 through 9, the precipitates were filtered immediately. Precipitates in 10 and 11 stood overnight, those in 12 through 17 about one hour, and 18 through 20 about three days.

In view of the extremely varied results and the inconsistencies among identical experiments, little can be said in the nature of a correlation. In those cases where precipitation was complete, however, the ratios of greater than three indicate that complexing may have occurred, since the theoretical ratio of IO_3^-:In^{+++} is 3:1. The experiments on this method were therefore discontinued.

Indium Oxalate: Moeller (38) has studied the reactions between indium ion and various soluble oxalates. He has found that in the case of sodium, potassium or ammonium oxalates, a precipitate was formed in which the

TABLE VI

Results of Experiments With Indium Iodate

Experiment	cc. KIO_3 Solution Added	Total Volume	Completeness of Precipitation	Iodate concentration after Precipitation	ratio $\frac{\text{moles } IO_3^- \text{ in ppt.}}{\text{moles } In^{+++} \text{ taken}}$
1	10	40	Incomplete	0.1f	3.78
2	10	50	Incomplete	.08	3.38
3	10	60	Incomplete	.07	3.05
4	25	40	Complete	.29	3.78
5	25	50	Complete	.23	3.39
6	25	60	Complete	.19	3.06
7	25	50	Complete	.23	3.20
8	25	50	Complete	.23	3.32
9	25	50	Complete	.23	3.38
10	25 *	60	Incomplete	.19	2.62
11	25 *	60	Incomplete	.19	2.95
12	30	50	Incomplete	.28	2.29
13	35	50	?	.33	2.22
14	40	50	?	.38	2.35
15	20 *	50	Incomplete	.20	2.23
16	25 *	50	Incomplete	.23	2.40
17	45 *	55	Incomplete	.39	2.65
18	15	50	Incomplete	.13	2.68
19	20	50	Incomplete	.18	2.92
20	25	50	Incomplete	.23	2.90

* $NaIO_3$ used

oxalate-indium ratio was 2:1 and that in the case of oxalic acid, the ratio was 1.5:1. No solubility data was given, but it was indicated that the compounds were slightly soluble in water.

Some experiments were performed to test the suitability of an insoluble indium oxalate for an analytical precipitation. Both oxalic acid and potassium oxalate were used, in excesses of 3 to 1 and 5 to 1. The precipitates were crystalline and showed a tendency to form supersaturated solutions. In no case was the indium precipitated completely.

The Ferricyanide-Iodide Method

Description of the analogous method for zinc: A volumetric determination of zinc, based upon the addition of excesses of potassium ferricyanide and potassium iodide, and iodometric titration of the liberated iodine, has been developed by Maun and Swift. (39) Briefly the method consists of buffering the zinc solution at a pH of about 3, adding the iodide and ferricyanide, allowing the solution to stand a few minutes, and then titrating with a standard $Na_2S_2O_3$ solution. The main reaction is:

$$2Fe(CN)_6^{\equiv} + 3I^- + 3Zn^{++} + 2K^+ \longrightarrow I_3^- + Zn_3K_2[Fe(CN)_6]_2$$

The result must be increased by a factor of 1.9%, but if the variables are controlled to a reasonable degree, results accurate to 0.1 - 0.2% can be obtained.

The method is based on the fact that ferricyanide ion will not oxidize iodide ion appreciably, and only slowly even then. Addition of a metal ion such as zinc, which forms an insoluble ferrocyanide, but not a ferricyanide, effectively raises the oxidation potential of the couple, and iodide will be oxidized until the zinc has been completely precipitated.

Indium behaves analogously with respect to these reactions and it was thought that the method might be applied to indium, to give a rapid precise volumetric determination.

Solutions: Buffering was done by a phthalate-biphthalate buffer. A saturated solution of potassium biphthalate was prepared by allowing an excess of the salt to stand in one liter of water for several hours, after which the solution was decanted and used.

0.10 formal solutions of potassium ferricyanide were prepared by dissolving the appropriate quantity of salt in water and storing the solution in a black lacquered bottle, kept in the dark.

Standard 0.1 formal indium solutions were prepared by weighing out calculated amounts of the 99.97% pure metal, dissolving it in acid, and diluting to one liter. Nitric acid was used at first, but on account of the possibility of oxidation by iodide by nitrate, sulfuric acid was later used. The amount of acid used was such that the final concentration was about 0.1 normal.

The sodium thiosulfate solutions were made up to be about 0.05 normal according to the method of Swift,(24) and standardized against potassium dichromate.

Preliminary Experiments: At least two possible sources of error exist. One is the oxidation of iodide ion by oxygen of the air, and the second is oxidation of iodide by ferricyanide. Both of these effects are minimized by Maun and Swift by buffering the solution to be titrated at a pH of about 3, since the potentials of both reactions are lowered by decreasing the acidity. The same buffer was used here, since the precipitation of hydroxide at a pH of 3.4(42) prevents the use of higher pH values. In order to obtain an idea of the rate of this reaction, two experiments were run in the same buffer containing potassium iodate and starch solution. 6 cc. of 1.0 normal sulfuric acid and 25 cc of saturated potassium biphthalate were diluted to 250 cc. The iodide concentrations were respectively 0.05 and 0.10 in the two experiments. After ten hours in the dark, no color was observed in the first and 0.03 cc. of 0.05 normal thiosulfate were needed to decolorize the second. Although the rate of oxidation here was slow, catalysis may occur in the actual titrations, so that not too much weight should be attached to these results.

More meaningful is the second set of experiments, in which the rate of oxidation of iodide by ferricyanide is observed. Buffered solutions, 0.05 and 0.10 formal in KI and 0.004 and 0.001 formal in $K_3Fe(CN)_6$ were prepared and starch added. No color was formed immediately or in 6 minutes, but at the end of 15 minutes, 0.02 cc of 0.05 normal thiosulfate was needed to decolorize the first and 0.04 cc. for the second. Thus if the solution to be titrated is permitted to stand more than 10 to 15 minutes an appreciable error may be introduced from this source. Maun and Swift recommend that the time of standing be five minutes. The end-point was found to fade fairly rapidly in all titrations performed here, presumably due to this oxidation, but the color change was quite definite and held for one or two minutes.

Procedure: It was decided to vary three quantities; the concentrations of KI and $K_3Fe(CN)_6$ and the time of standing prior to titration. A set of three concentrations each of the two salts was used as shown in Table VII. The numbers within the squares will be used to designate the corresponding results. The time factor was varied by performing titrations after allowing successively 0, 5, 10, and 15 minutes to elapse after mixing. In some cases longer periods were used.

TABLE VII

Concentration Scheme for Preliminary Experiments

Conc. of KI \ Conc. of $K_3Fe(CN)_6$	.0005 f.	.0010 f.	.005 f.
.01 f.	1	2	3
.05 f.	4	5	6
.10 f.	7	8	9

Numbers 1 through 9 are experiment numbers

10 cc. of indium solution were pipetted with a calibrated pipet into a 500 cc. Erlenmeyer flask. 25 cc. of the phthalate solution, 6 cc. of 1.0 normal H_2SO_4 and 100 to 150 cc. of distilled water were added. The proper amount of KI was added and finally a measured volume of $K_3Fe(CN)_6$. Sufficient water had been previously added to make a total volume of 250 cc. The solutions were swirled and put in the dark for the required time, after which they were titrated with 0.05 normal $Na_2S_2O_3$ from a calibrated buret, using starch indicator. Usually from 15 to 20 cc. of thiosulfate were needed.

During the first few titrations, the ferricyanide was run in from a buret, and the results were several percent low. After this was noted, the ferricyanide was measured out and added all at once. The results were then in the neighborhood of the actual values, and no other variations were tried.

Two identical titrations were always made and the results averaged. In case poor agreement between the two was obtained, more titrations were made and an average calculated.

In one titration, pH readings were taken with a Beckman pH meter. The results are as follows: (total volume 250 cc.)

pH of buffer	2.83
pH of buffer after adding indium solution	2.60
pH just before titration	2.74
pH at end-point	2.78

Results: The results of this set of experiments are shown in Table VIII. It will be seen that there is little agreement shown here, although in some cases, the change of one variable does not cause a large change in the results. Experiment Number 5, which contained the intermediate amounts of both $K_3Fe(CN)_6$ and KI, seemed to show as little change as any, and it was decided to investigate other compositions in this region. To do this, the KI

TABLE VIII

Results of Preliminary Experiments
.999 millimoles In^{+++} taken in all experiments

Experiment	Conc. I^-	Conc. $Fe(CN)_6^{\equiv}$	Time of Standing	Millimoles In found
#1	.01 f.	.0005	0	-
	.01 f.	.0005	5	.944
	.01 f.	.0005	10½	.949
	.01 f.	.0005	15	.948
	.01 f.	.0005	120	.945
#2	.01 f.	.001	0	-
	.01 f.	.001	5	.943
	.01 f.	.001	10	.960
	.01 f.	.001	15	.958
	.01 f.	.001	120	.967
#3	.01 f.	.005	0	.971
	.01 f.	.005	5½	.985
	.01 f.	.005	11	.994
	.01 f.	.005	15	.996
	.01 f.	.005	30	1.013
	.01 f.	.005	120	1.002
#4	.05 f.	.0005	0	.960
	.05 f.	.0005	5	.964
	.05 f.	.0005	10½	.984
	.05 f.	.0005	15	.988
	.05 f.	.0005	120	1.025
#5	.05 f.	.001	0	.971
	.05 f.	.001	5	.970
	.05 f.	.001	10	.994
	.05 f.	.001	15½	1.007
	.05 f.	.001	30	1.015
	.05 f.	.001	120	1.038
#6	.05 f.	.005	0	.992
	.05 f.	.005	5	1.005
	.05 f.	.005	10	1.038
	.05 f.	.005	15½	1.039
	.05 f.	.005	120	1.078
#7	.10 f.	.0005	0	.972
	.10 f.	.0005	6	.981
	.10 f.	.0005	10	1.025
	.10 f.	.0005	15	1.006
	.10	.000f	30	1.018
#8	.10 f.	.001	0	.976
	.10 f.	.001	5½	.996
	.10 f.	.001	10	1.009
	.10 f.	.001	15½	1.017
#9	.10 f.	.005	0	-
	.10 f.	.005	5	1.034
	.10 f.	.005	10½	1.041
	.10 f.	.005	15	1.053

concentration was maintained at 0.05 formal, while the ferricyanide concentration and the reaction time were varied. These results are shown in Table IX and indicate the existence of a small region in which reasonably constant values in the neighborhood of the correct result are obtained.

The effect of change of KI concentration was determined in Series II, III, and IV of experiments. The KI concentration was kept at 0.074 formal in Series II, and 0.028 formal in Series III, and 0.057 formal in Series IV. The results of these experiments are shown in Table V.

As mentioned previously, there seems to be a small region of concentrations in which reasonably constant results were obtained. In Series I, Table IV, the concentrations 5B, 5D, and 5F show variations of about one percent or less. About the same variation is observed for concentration B, D and F in Series II and IV, which contained KI at a higher concentration. In series III, where the KI concentration was only 0.028 formal, low results were obtained in the only two experiments performed. In general, it may be stated that one factor, possibly two, may be varied simultaneously without affecting too greatly the results, but no more. This necessarily restricts the allowable range of the variables.

It should be repeated that the results in the tables are the average of two or more titrations. These individual results quite often agreed to 0.1% but more often disagreed by several tenths of a percent. Even when several titrations were made, the results were inconsistent on the order of one-half to one percent.

In summary, then, for quantities of indium, in the vicinity of one millimole, or 115 milligrams, results accurate to about one percent have been obtained. The iodide concentration has been kept between 0.05 and 0.075 formal, the ferricyanide between 0.002 and 0.003 formal, the reaction time between five and fifteen minutes, and the volume of solution constant at 250 cc.

TABLE IX

Results of Series I, II, III and IV Experiments

Series I
Concentration of KI = .05 f.
.998 millimoles In^{+++} taken
millimoles In^{+++} found in each experiment

Experiment #	#4	#5	#5C	#5A	#5D	#5B	#5F	#5E	#5G	#5H	6
cc .10 f. $K_3Fe(CN)_6$ / Time	9.3	10.5	11.3	12	13	14	15	16	17	18	20.5
5 minutes				.985	.992	.997	.995	.999	.994	1.006	
10 minutes	.984	.994	.989	1.003	1.000	.999	.998	1.003			1.038
15 minutes	.988	1.007	.992	1.003	1.002	1.002	1.012	1.018			1.039

Series II
Concentration of KI = .074 f.
* .998 millimoles In^{+++} taken
.999 millimoles In^{+++} taken

Experiment # / Time	#5C	#5A	#5D	#5B	#5F	#5E
5 minutes	.989	.984	.985	1.009		
10 minutes	.985	1.005*	1.007*	1.002*	1.007*	1.010

Series III
Concentration of KI = .028 f.
.999 millimoles In^{+++} taken

Experiment # / Time	#5A	#5D
10 minutes	.975	.980

Series IV
Concentration of KI = .057 f.
.999 millimoles In^{+++} taken

Experiment # / Time	#5A	#5D	#5B	#5F	#5E
10 minutes	.993	.998	.995	1.004	1.012

Discussion: In its present state, this application of iodometry to the determination of indium cannot be considered of very great value, principally for two reasons. The first is that the quantities of indium are usually unknown and therefore the exact quantities of reagents to be added will be unknown. Unless the indium concentration were approximately known, several titrations might be needed in order to determine it. The second reason is that the effect of other ions on the equilibria is unknown. Usually indium is separated as the sulfide or hydroxide and redissolved in acid, so that no interfering ions would be present. However, at least one, an alkali or ammonium ion would be introduced in adjusting the acid concentration prior to titration. The effect of these ions should be known.

The cause of the inherent inaccuracies here is not known. There are two possibilities, however. One is that adsorption on the surface of the precipitate of potassium indium ferrocyanide may occur. Adsorption of either indium or ferrocyanide ions would give rise to errors. If this were the case, a possible remedy would be to add some preferentially adsorbed ion to the solution. Here again, however, the effect of the ion on the equilibria would have to be studied, and since most ferrocyanides are insoluble, added complications would arise. The second possibility is that in a complicated compound such as the precipitate is, small amounts of other similar compounds may be precipitated; that is, ones having a different ratio of indium to ferrocyanide. The surprising accuracy of the results in the zinc titration can possibly be ascribed to a saturated solid solution of the compound $Zn_2Fe(CN)_6$ in the compound $Zn_3K_2[Fe(CN)_6]_2$.(40) A similar situation may occur here, but with much wider solid solution range. It will be recalled that Bray and Kirschman, in their potentiometric determination, found that the solution had to be of low ionic strength, otherwise sharp end-points were not obtained. It would be difficult to decrease greatly the ionic strength in this procedure, but by using larger volumes, or scaling the quantities down for determinations of say 10 milligrams of indium, some improvement might be realized.

REFERENCES

1. Fr. Heusler, Stark, and Haupt, Verh. deuts. phys. Ges. 5, 219, (1903)
2. See for example Bates, "Modern Magnetism", Cambridge, p. 240.
   Also Messkin & Kussman, "Die Ferromagnetische Legierungen", Berlin,
   J. Springer, p. 142-144.
3. Bradley & Rogers, Proc. Roy. Soc. 144, 340, (1934).
4. O. Heusler, Ann. d. Phys. 19, 155, (1934).
5. Valentiner & Becker, Zeit. f. Phys. 83, 371, (1933).
6. O. Heusler, Zeit, f. Metallkunde, 25, 274, (1933).
7. Persson, Zeit. f. Phys. 57, 115, (1929).
8. Carapella & Hultgren, Metals Technology, T. P. 1405 (Oct. 1941).
9. Grinstead & Yost, Phys. Rev. 75, 984, (1949).
10. Valentiner, Naturwiss. 4, 123, (1947).
11. Coles, Hume-Rothery & Myers, Proc. Roy. Soc. A 196, 125, (1949).
12. Van Dusen & Dahl, Bur. Stds. J. Rsch. 39, 291, (1947).
13. Gayler, J. Iron & Steel Inst. 115, #1, 393, (1927).
14. Swanger & Caldwell, Bur. Stds. J. Rsch. 6, 1131, (1931), R. P. 327.
15. Roeser & Wensel, Bur. Stds. J. Rsch. 10, 275, (1933), R. P. 530.
16. Roeser, Dahl & Gowens, Bur. Stds. J. Rsch. 14, 239, (1935), R. P. 767.
17. Roeser & Wensel, Bur. Stds. J. Rsch. 14, 247, (1935), R. P. 768.
18. Latimer & Hildebrand, "Reference Book of Inorganic Chemistry", Macmillan,
    P. 369.
19. Mellor, "Comprehensive Treatise on Inorganic & Theoretical Chemistry",
    Longmans, Vo. XII, p. 221-2.
20. Hay, White & McIntosh, J. West Scot. Iron & Steel Inst., 42, pt. 6, 99, (1935).
21. Bates, "Modern Magnetism", Cambridge, p. 259
22. Dean, Long, Graham, Potter, & Hayes, Trans A.S.M. 34, 443, (1945).
23. Weibke & Eggers, Z. anorg. allgem. chem. 220, 273, (1934).
24. Swift, "A System of Chemical Analysis", Prentice-Hall, p. 244.

25. Thiel & Koelsch, Z. anorg. allgem. Chem. 66, 288, (1910).

26. Hope, Ross & Skelly, Analyt. Chem. 8, 51, (1936).

27. Hillebrand & Lundell, "Applied Inorganic Analysis", Wiley.

28. Bates, Proc. Phys. Soc. 43, 87, (1931).

29. Weiss, J. de Phys., Ser. 4. 6, 661, (1907).

30. Stoner, "Magnetism & Matter", Methuen, p. 383.

31. Néel, Journ. de Phys. 5, 104, (1934).

32. Hume- Rothery, Raynor, Reynolds & Packer, J. Inst. Metals. 66, 209-39 (1940), Paper No. 876.

33. A. S. M. Metals Handbook, 1948 ed., 1176.

34. Hames & Eppelsheimer, Nature, 162, 968, (1948).

35. Belskaya, J. Applied Chem. U.S. S. R. 13, 470, (1940).

36. Bray & Kirschman, J. A.C.S. 49, 2739, (1927).

37. Ensslin & Dreyer, Z. anorg. allgem. Chem. 250, 199, (1942).

38. Moeller, J. A.C.S. 62, 2444, (1940).

39. Maun & Swift, Iodometric Determination of Zinc. Anal. Chem. 21, 798, (1949).

40. Personal Communication from Dr. E. H. Swift.

41. Bates, "Modern Magnetism," pp. 233-38.

42. Moeller, J.A.C.S. 63, 2525, (1941)

43. Ewing, "Magnetic Induction in Iron and other Metals", The Electrician Publishing Co. London.

44. Bates, L. F., "Modern Magnetism", Cambridge, pp. 375-78.

45. Hume-Rothery, Reynolds and Raynor, J. Inst. Metals 66, 191, (1940) Paper no. 875.

46. Laves & Wallbaum, Z. Angew. Mineral, 4, 17, (1942).

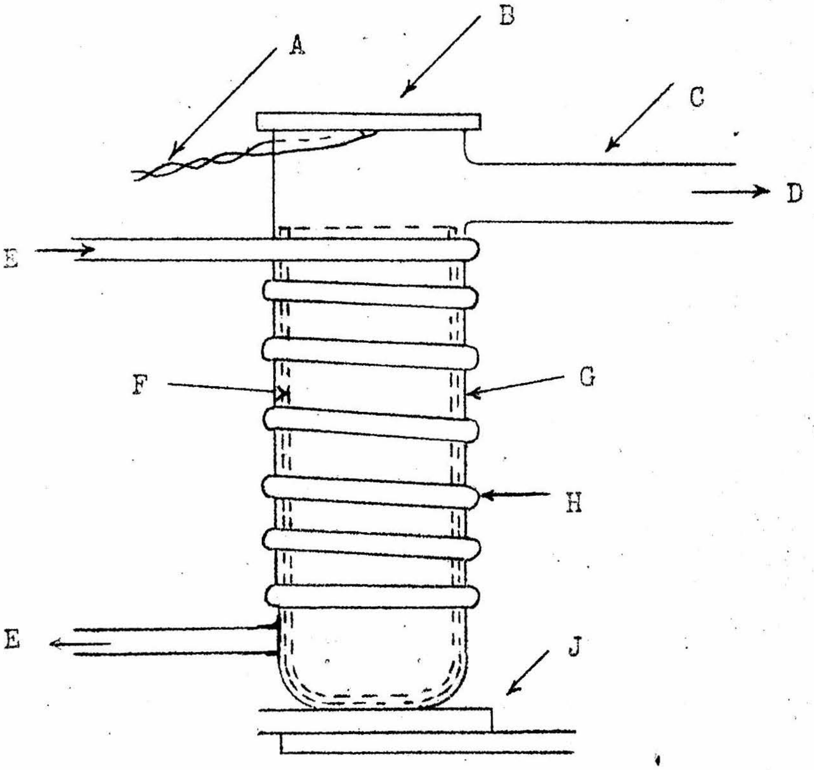

A Thermocouple leads

B Pyrex plate

C 35 mm pyrex tubing

D Vacuum & gas connection

E Cooling water

F Inner pyrex tube

G 61 mm pyrex furnace tube

H Copper heating coil

J Transite support

Fig. 1. External view of induction furnace and connections.

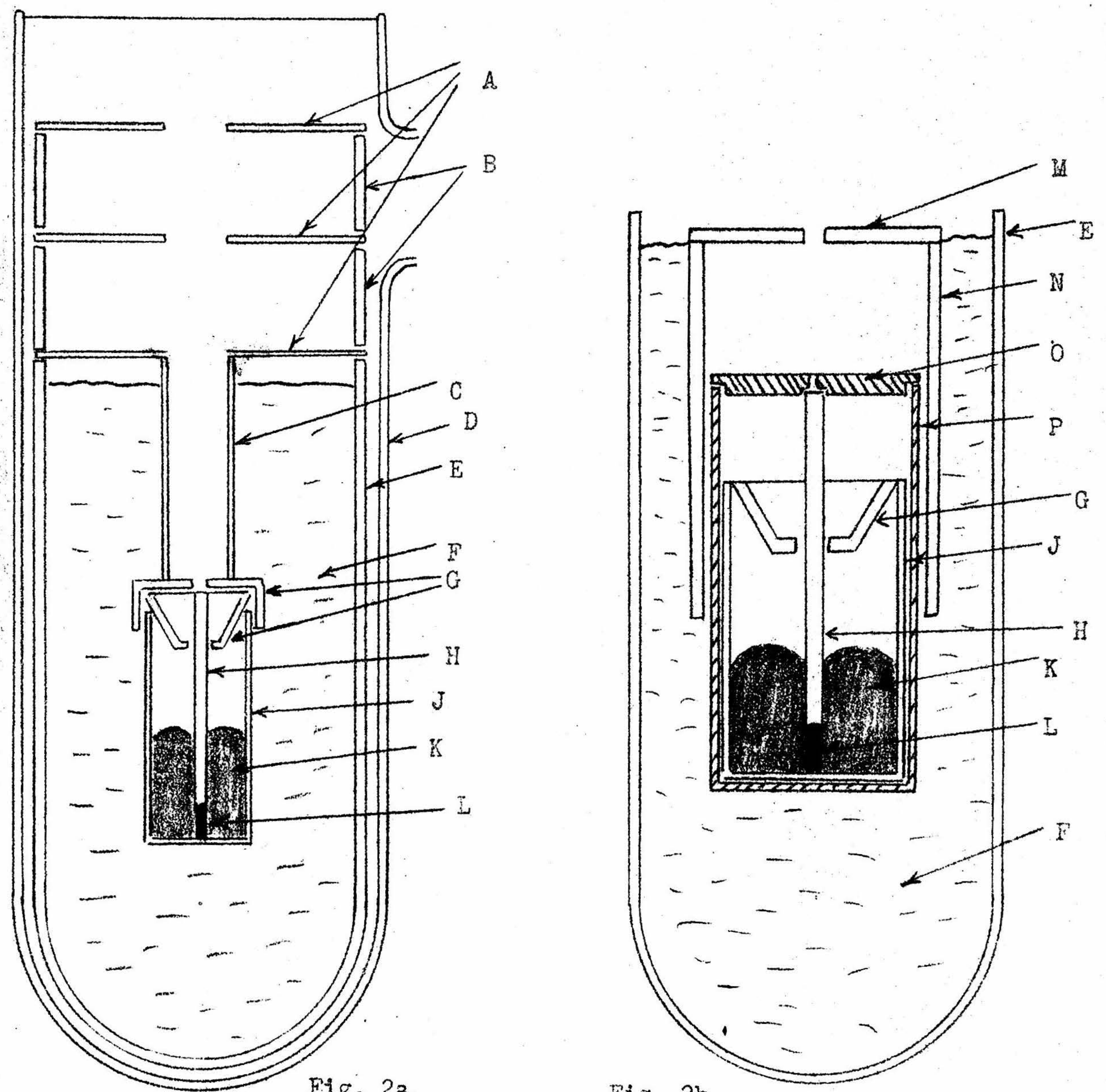

Fig. 2a.

Fig. 2b.

A	Asbestos or mica discs
B	Pyrex spacers
C	Alundum tube
D	Pyrex furnace tube
E	Inner pyrex tube
F	Zircon or zirconia powder
G	Alundum covers
H	Thermocouple protection tube
J	Alundum crucible
K	Alloy
L	Magnesia packing
M	Zircon disc
N	Zircon tube
O	Steel or graphite cover
P	Steel or graphite crucible

Fig. 2. Sections of induction furnace.

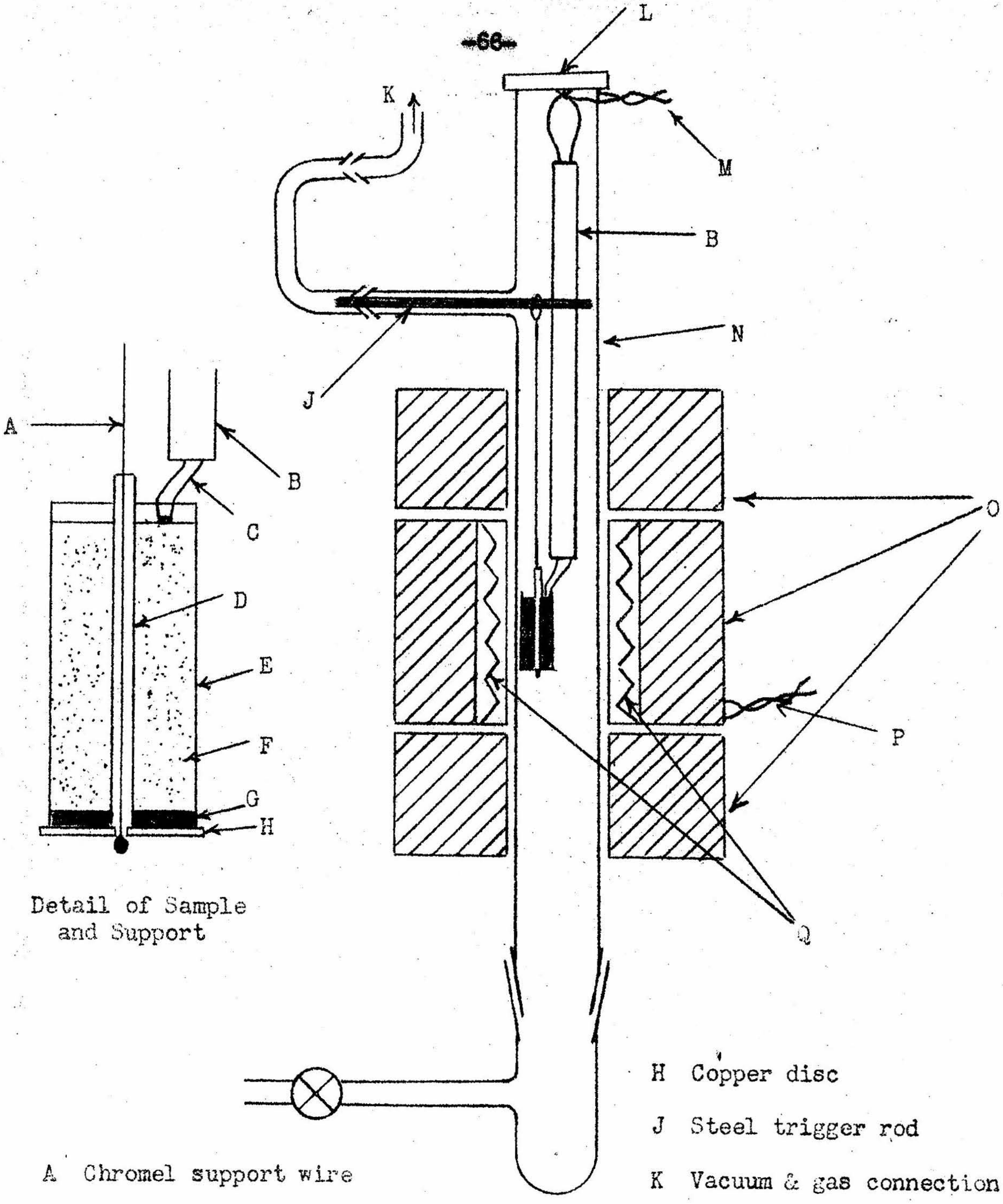

Detail of Sample and Support

A	Chromel support wire
B	Thermocouple insulator
C	Thermojunction
D	Porcelain protection tube
E	Alundum cylinder
F	Alloy
G	Magnesia packing
H	Copper disc
J	Steel trigger rod
K	Vacuum & gas connection
L	Pyrex disc
M	Thermocouple leads
N	Quartz furnace tube
O	Thermal insulation
P	Heater leads
Q	Heater windings

Fig. 3. Section of annealing furnace.

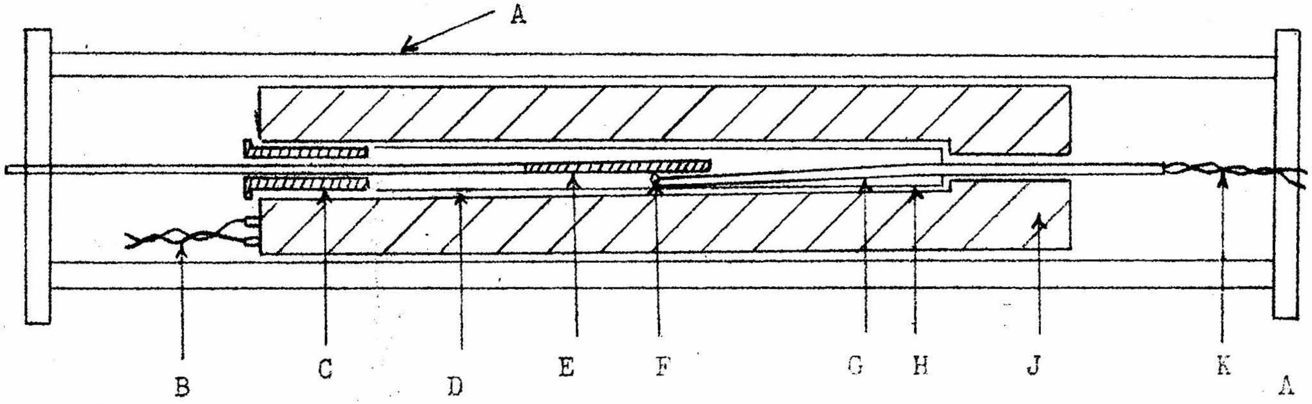

4a. Section thru solenoid

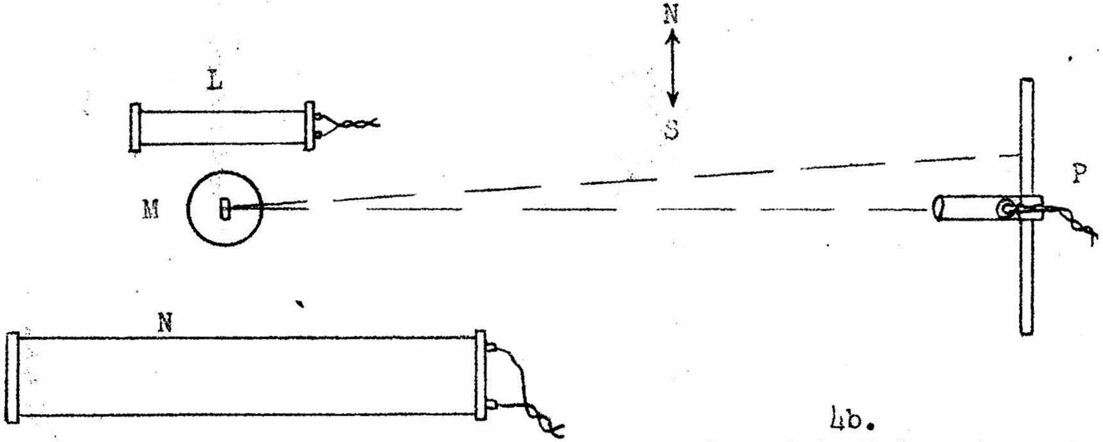

4b.
Geometrical layout

Fig. 4. Curie point apparatus.

A	Solenoid winding
B	Heater leads
C	Asbestos plug
D	Heater winding space
E	Pyrex sample holder & sample
F	Thermojunction
G	Thermocouple tube
H	Copper furnace tube
J	Asbestos insulation
K	Thermocouple leads
L	Balancing coil
M	Magnetometer
N	Solenoid
P	Lamp and scale

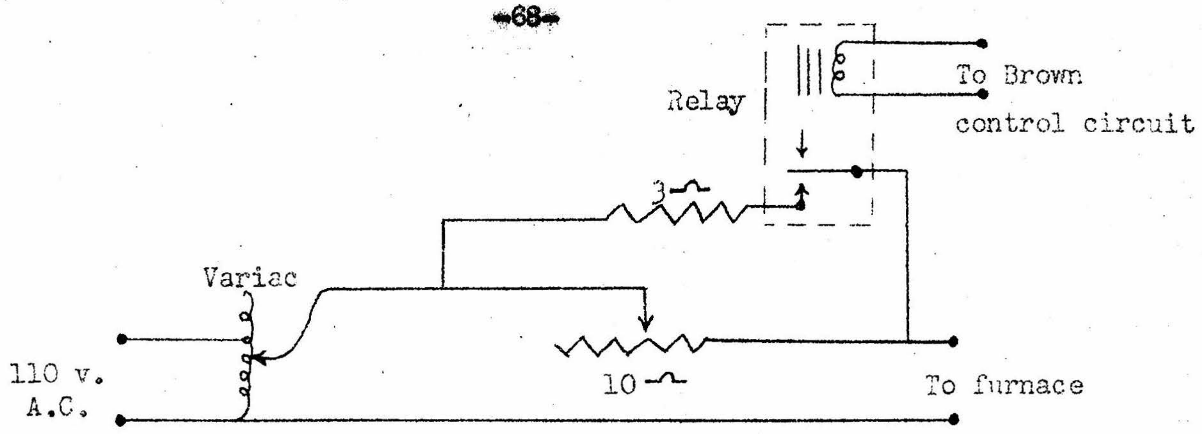

Fig. 5a. Annealing furnace control and heating circuit.

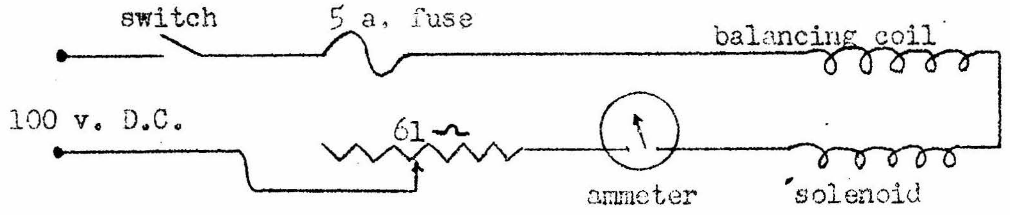

Fig. 5b. Curie apparatus magnetizing circuit.

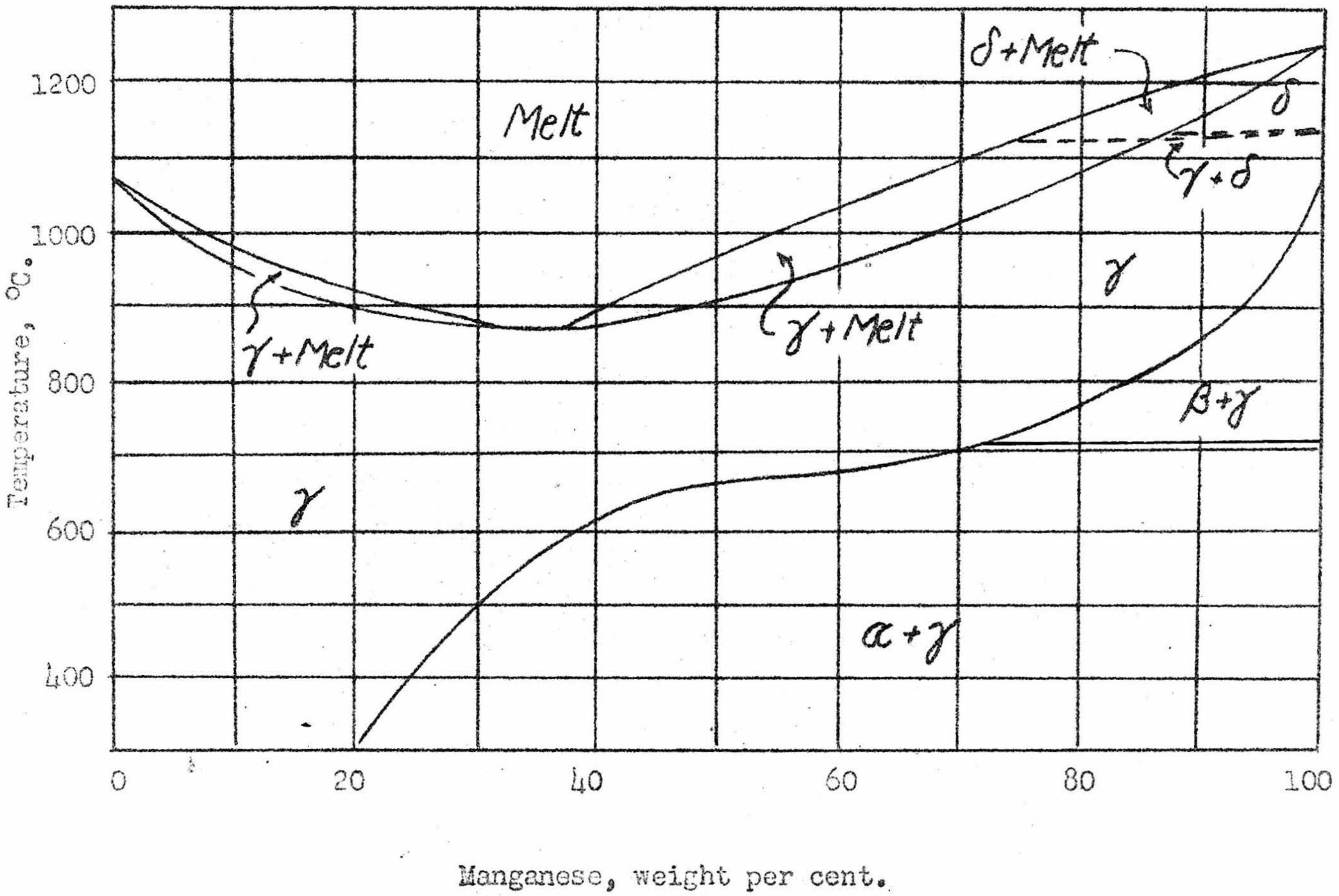

Fig. 6. Copper-Manganese equilibrium diagram. (Dean, Long, Graham, Potter & Hayes)

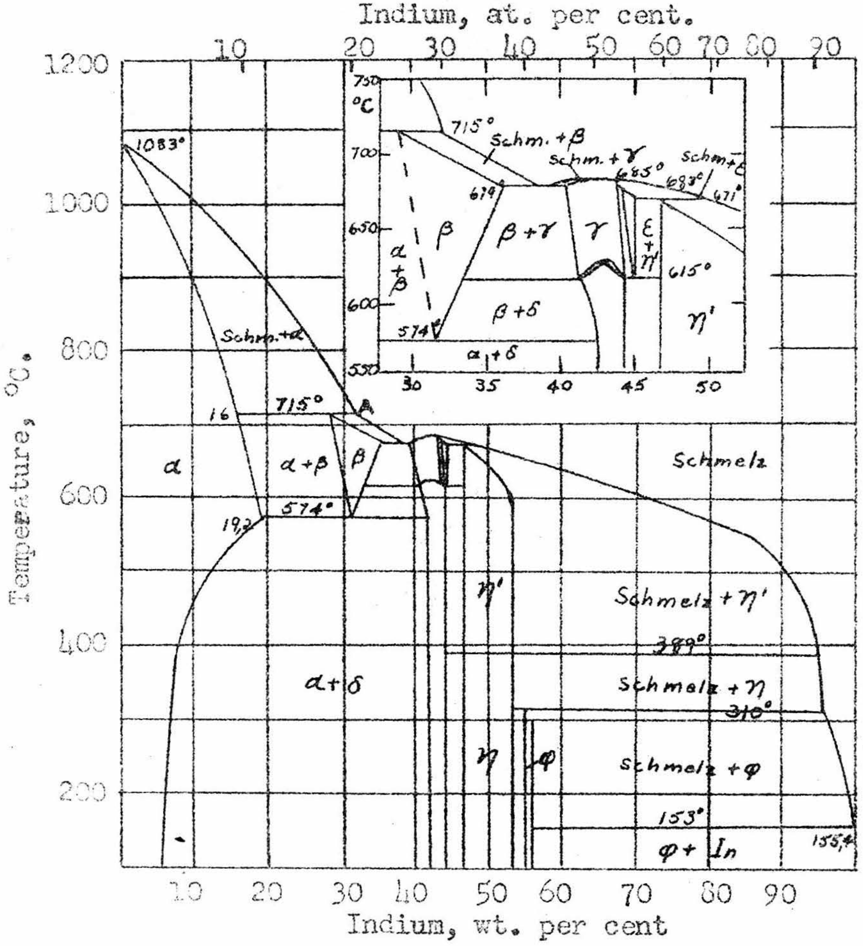

Fig. 7. Copper-Indium equilibrium diagram. (Weibke & Eggers)

Figures refer to liquidus temperatures of individual alloys. Long dotted line is the α-β peritectic line; shorter one is β-γ eutectic line.

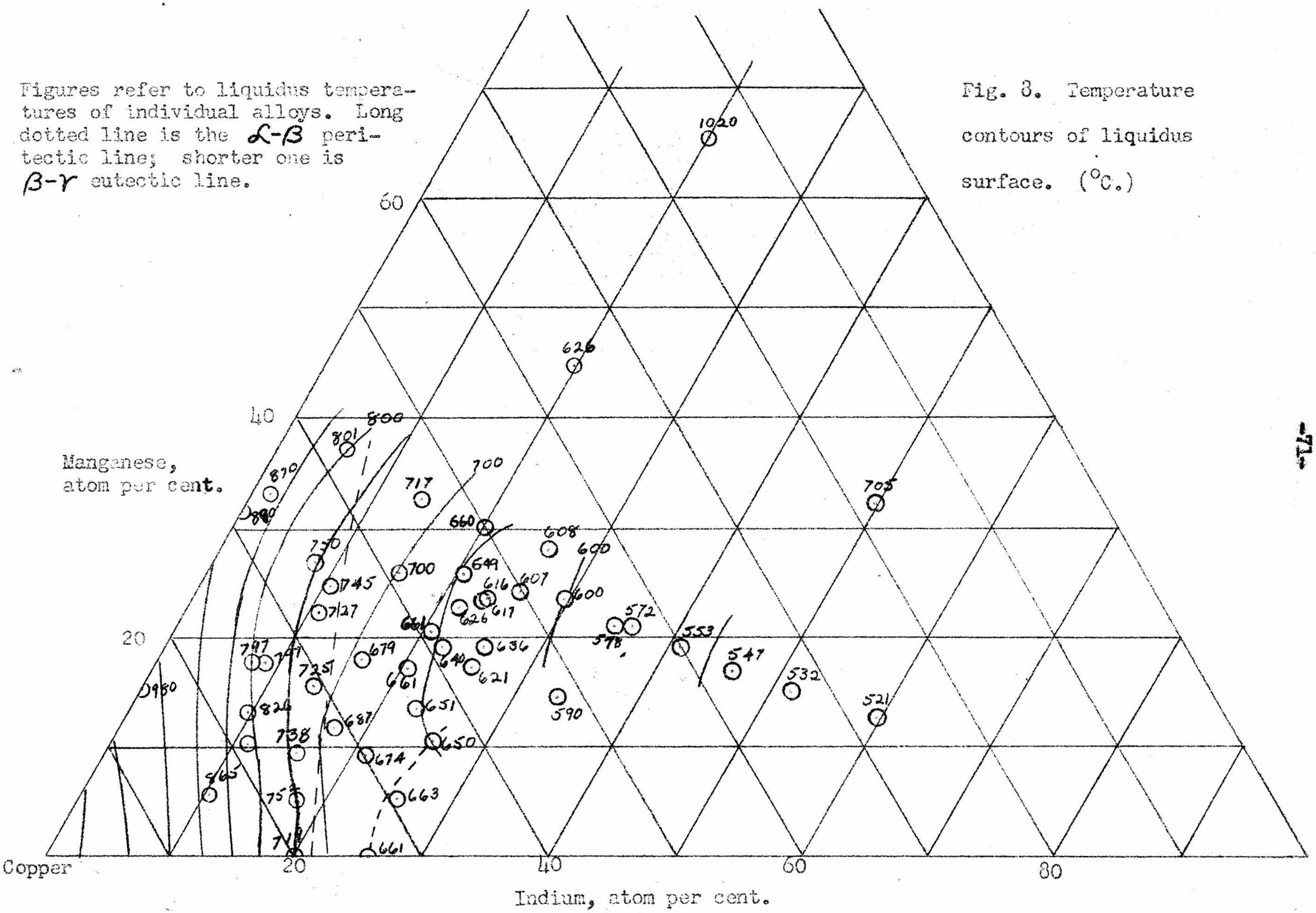

Fig. 8. Temperature contours of liquidus surface. (°C.)

Numbers are alloy designations. Phase boundaries in broken lines; $\alpha-\beta$ peritectic and $\beta-\gamma$ eutectic in full lines.

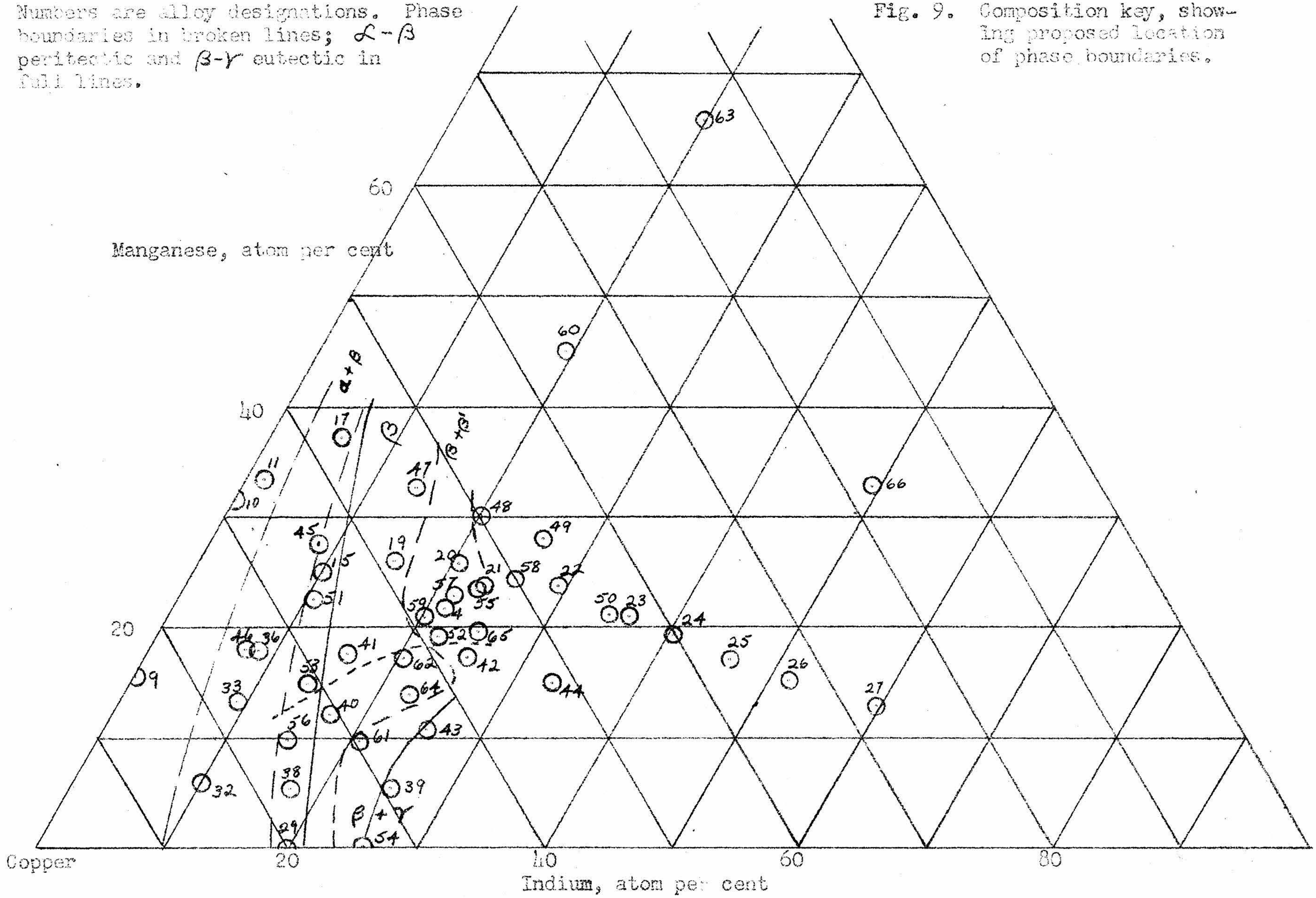

Fig. 9. Composition key, showing proposed location of phase boundaries.

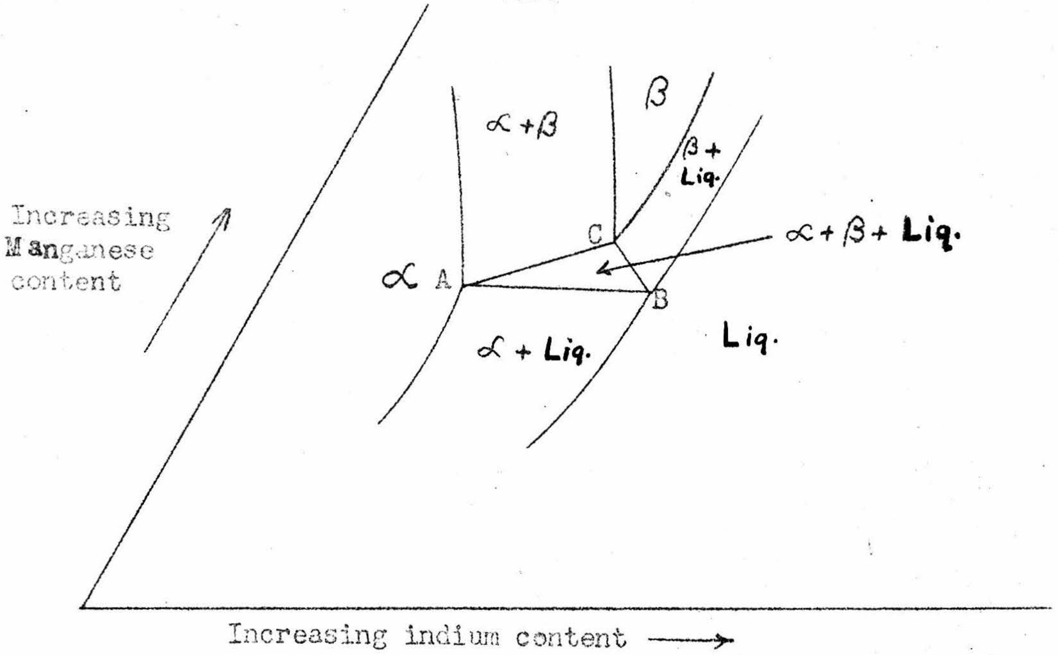

Fig. 10a. Isothermal section at about 730° C. thru composition-temperature diagram.

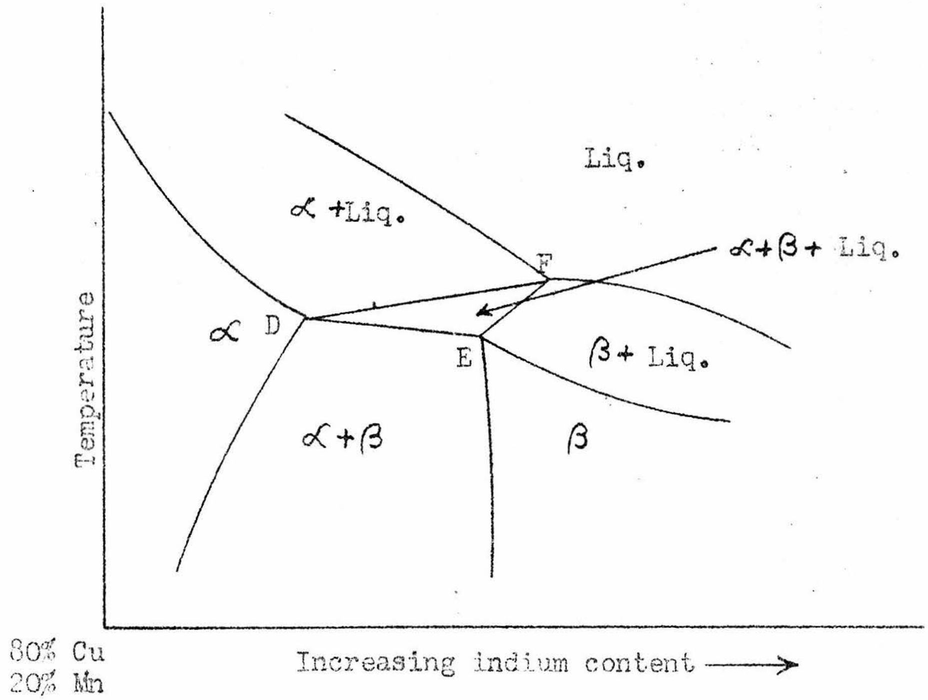

Fig. 10b. Section thru ternary composition-temperature diagram at about 20 atom per cent manganese.

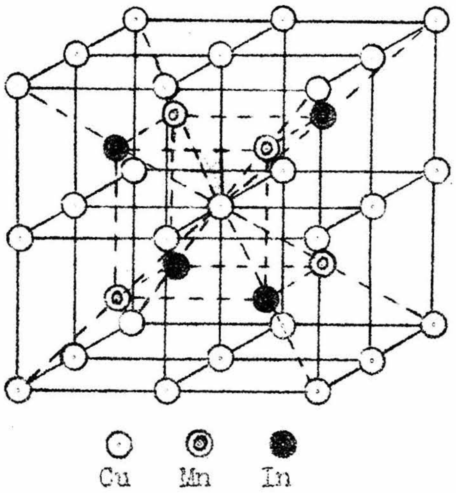

Fig. 11a. Structure of alloys in the vicinity of the composition Cu_2MnIn. (Hume-Rothery)

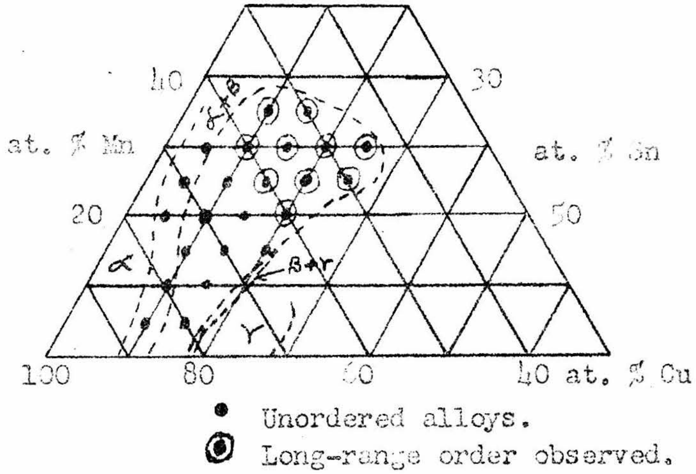

Fig. 11b. β-phase region in system Cu-Mn-Sn. (Carapella & Hultgren)

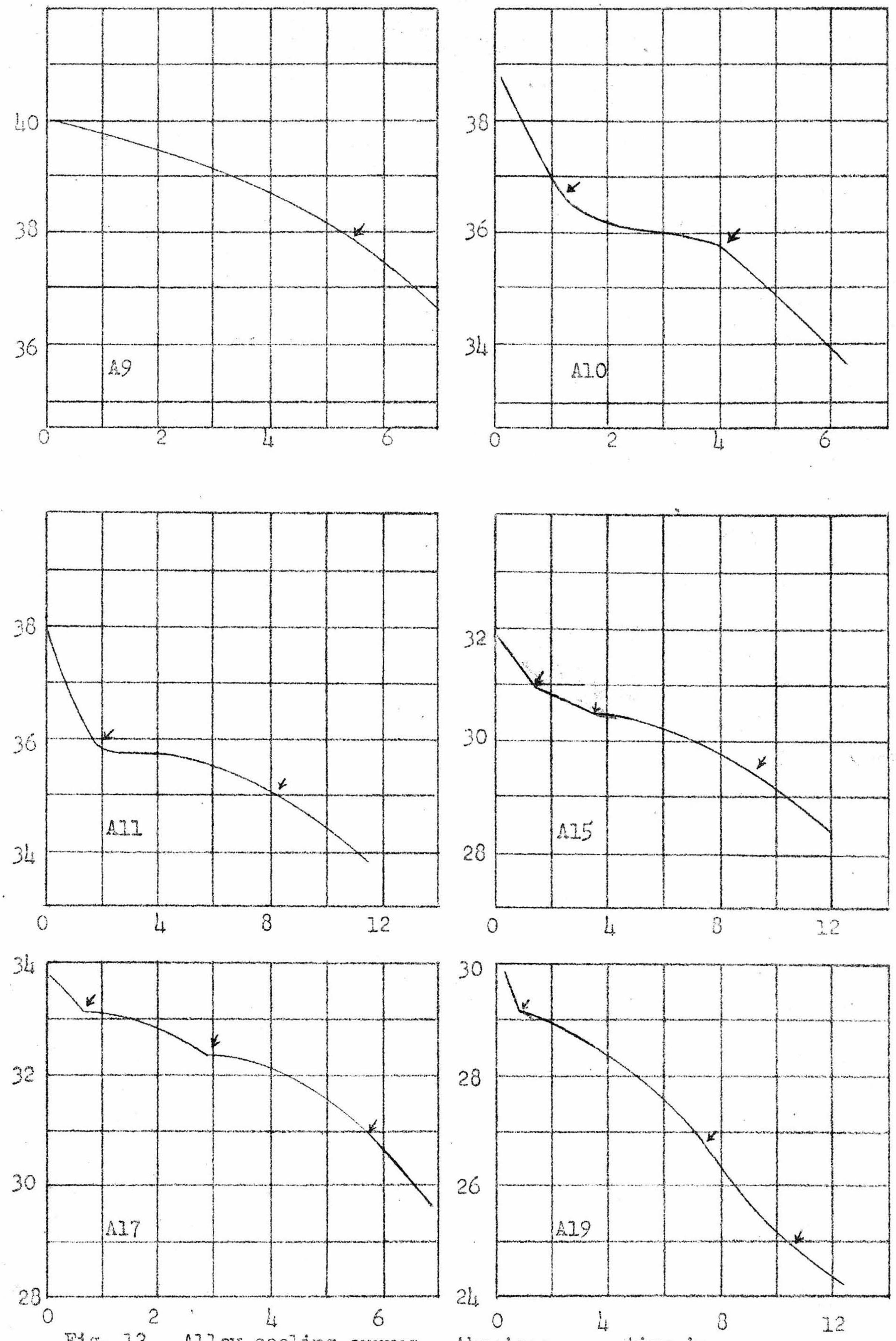

Fig. 12. Alloy cooling curves. Abscissae are time in minutes, ordinates are thermal emf in millivolts.

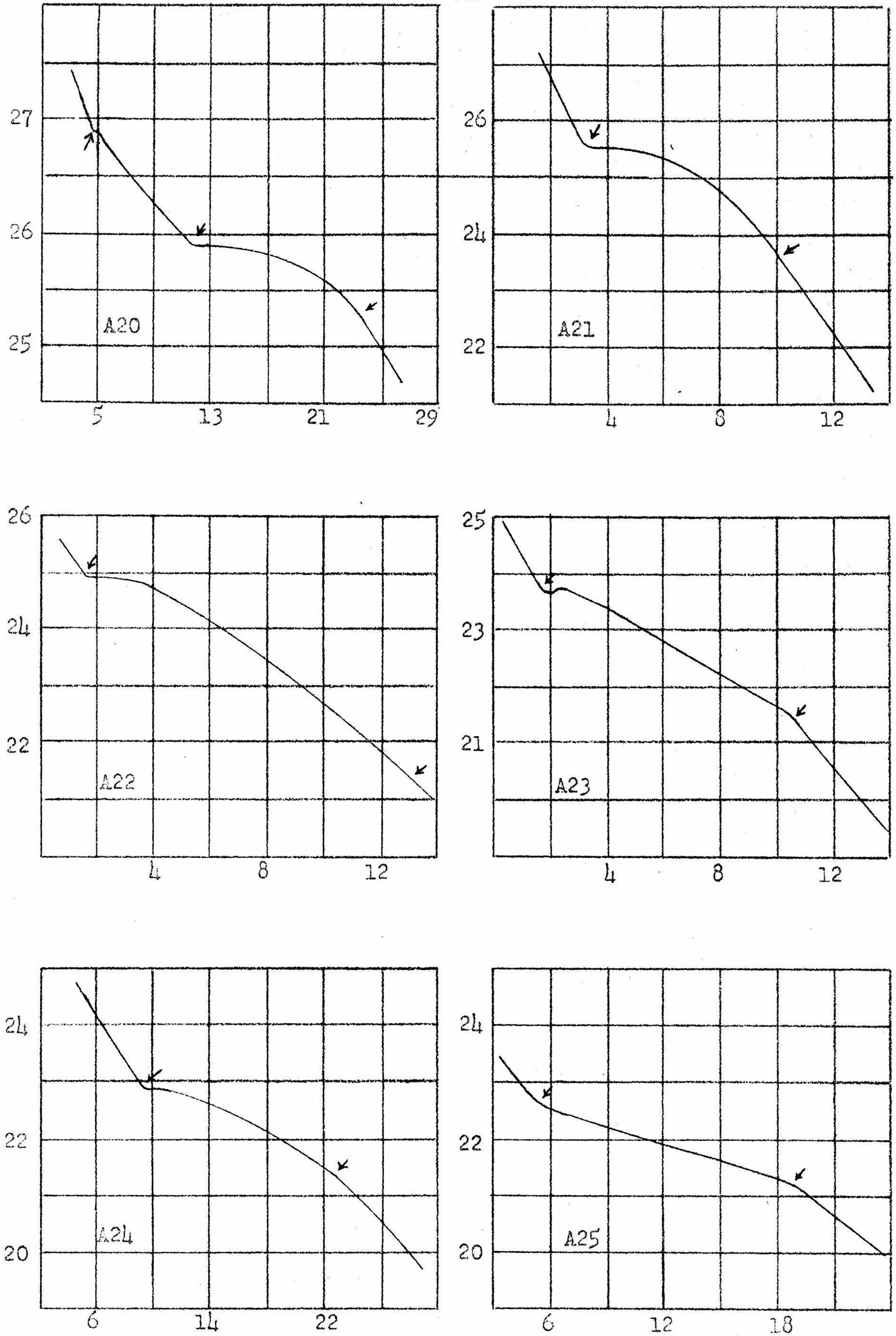

Fig. 13. Alloy cooling curves. Abscissae are time in minutes, ordinates are thermal emf in millivolts.

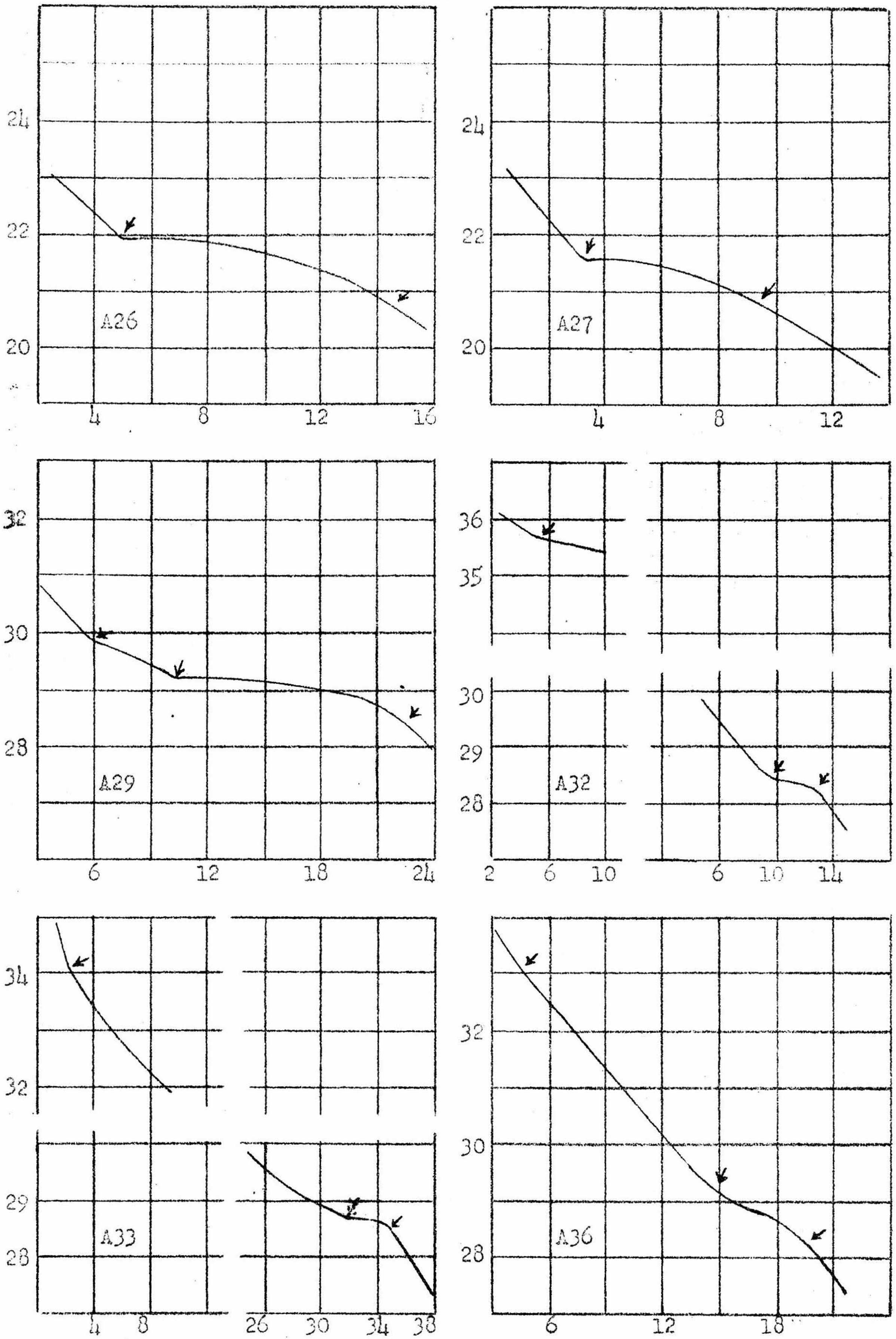

Fig. 14. Alloy cooling curves. Abscissae are time in minutes. Ordinates are thermal emf in millivolts.

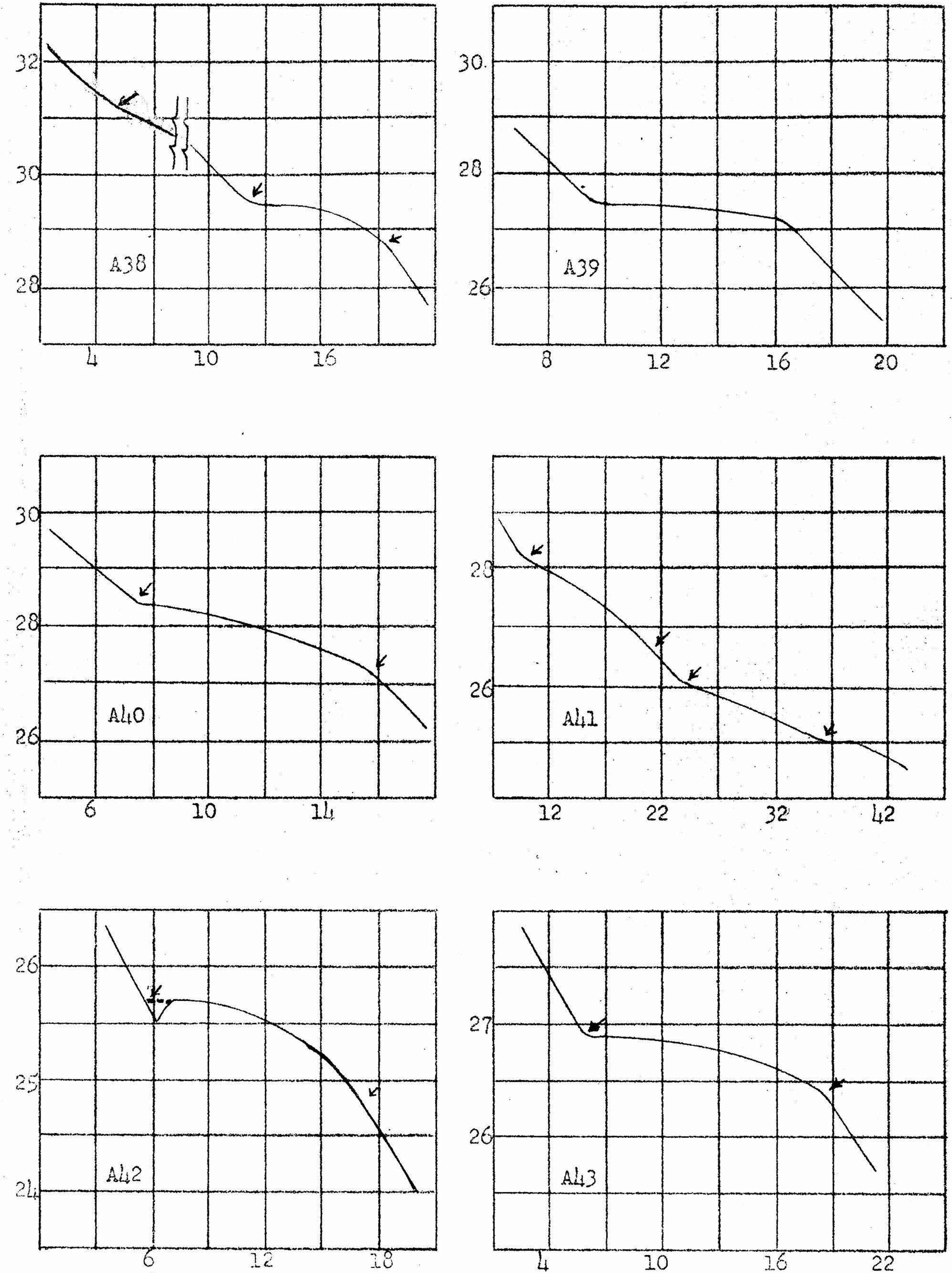

Fig. 15. Alloy cooling curves. Abscissae are time in minutes, ordinates are thermal emf in millivolts.

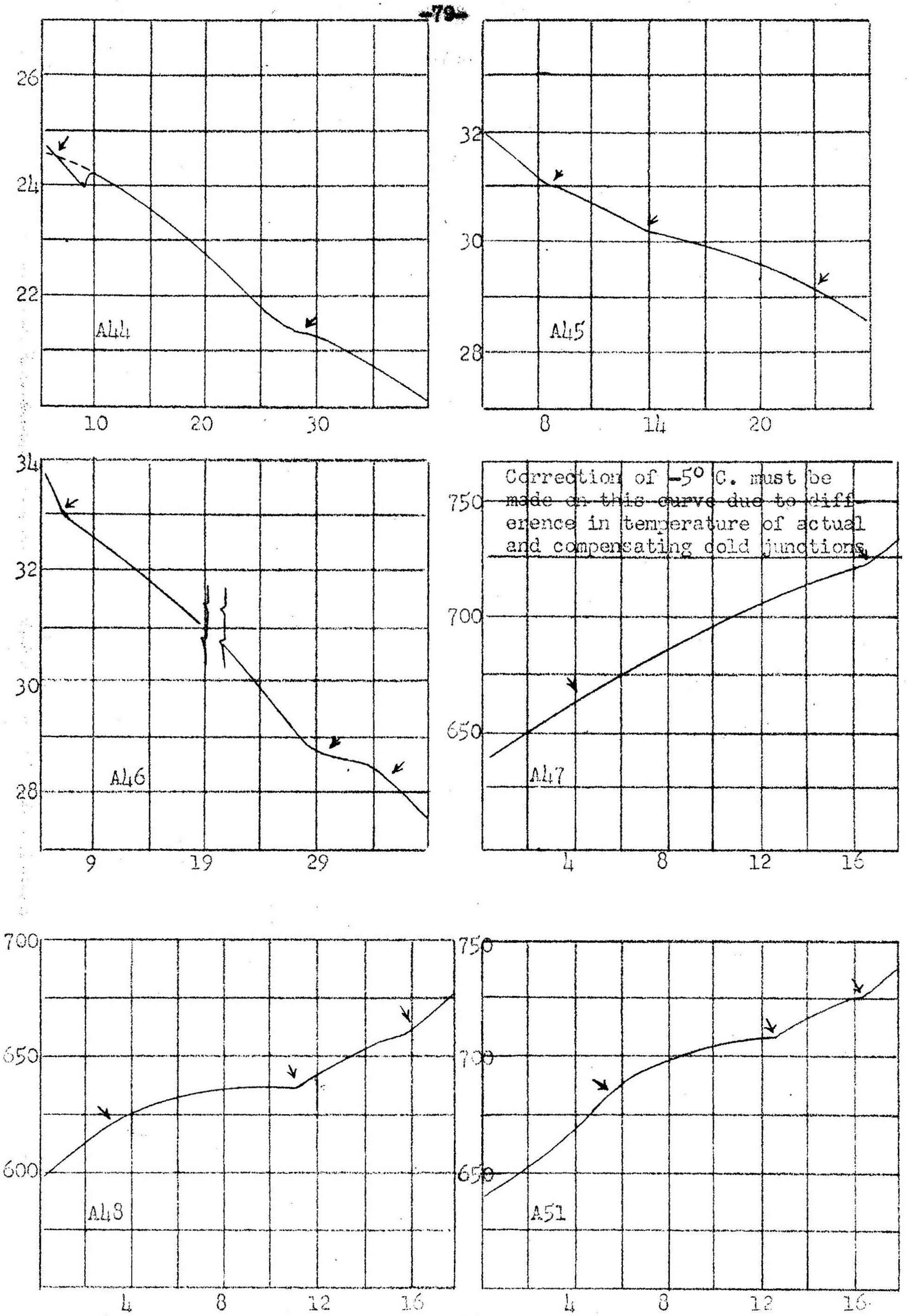

Correction of -5° C. must be made on this curve due to difference in temperature of actual and compensating cold junctions.

Fig. 16. Alloy cooling curves. Abscissae are time in minutes. Ordinates for A44, A45, A46 are thermal emf in millivolts, ordinates for A47, A48, A51 are temperature in degrees C.

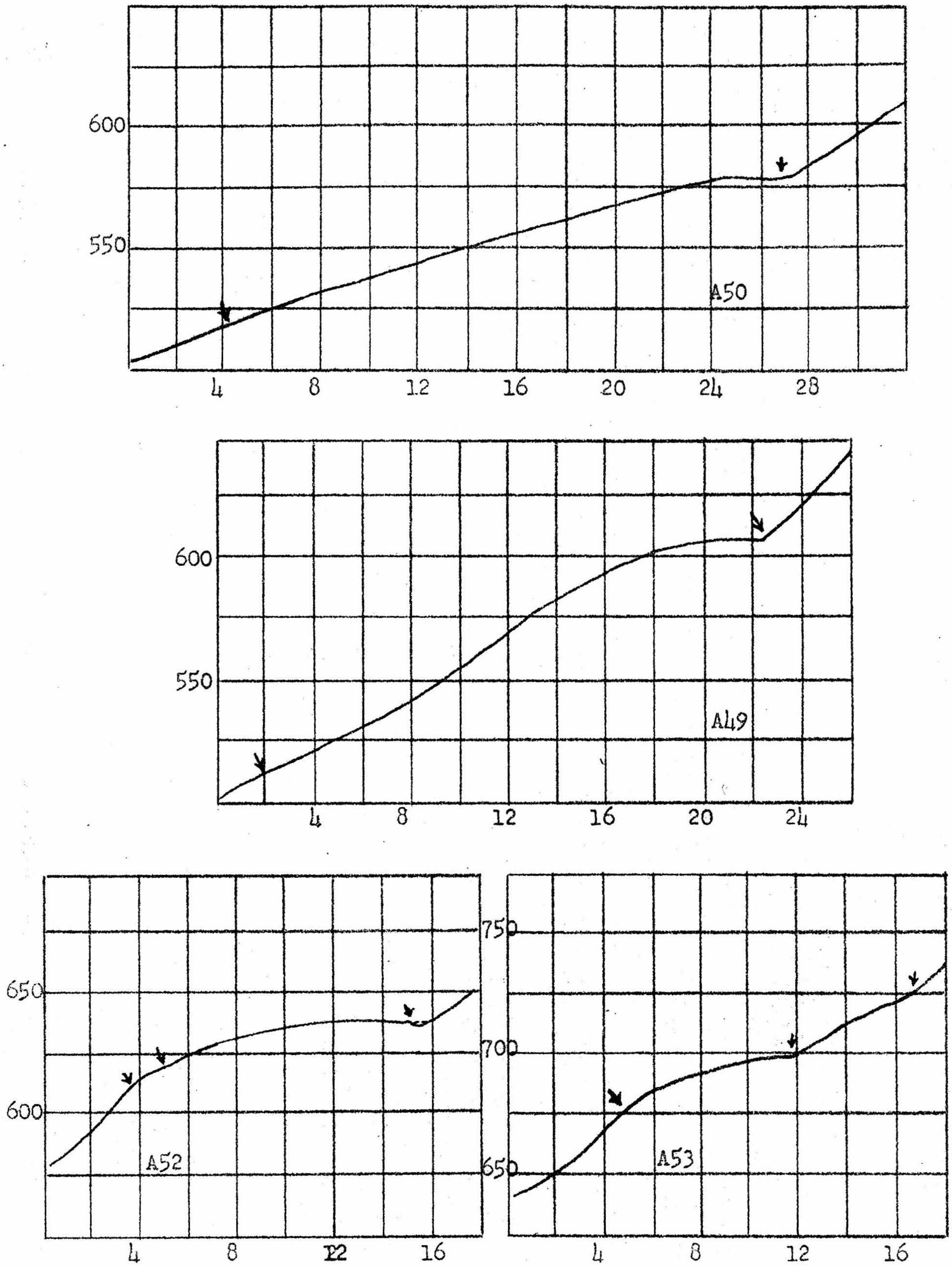

Fig. 17. Alloy cooling curves. Abscissae are time in minutes, Ordinates are temperature in degrees C.

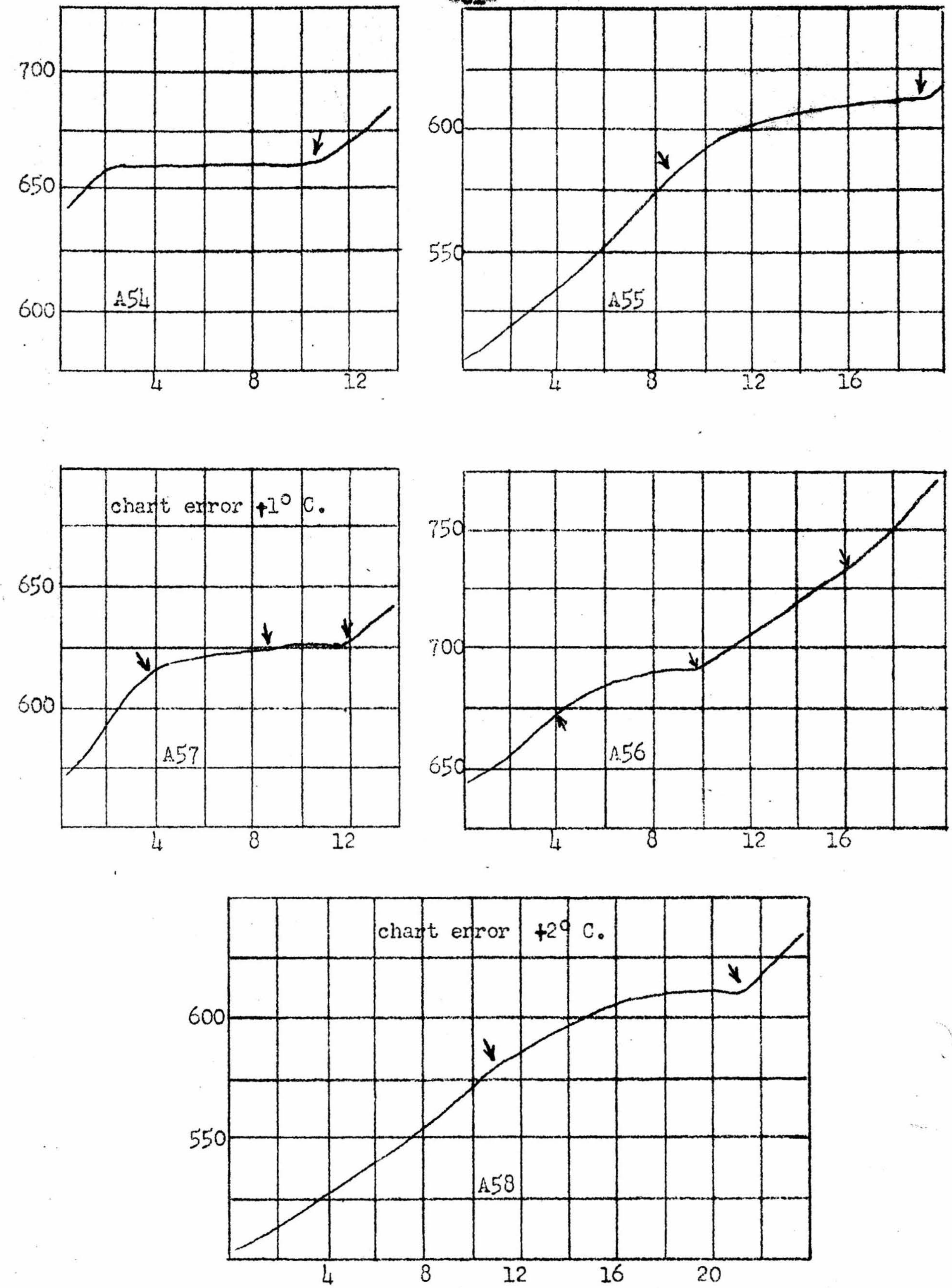

Fig. 18. Alloy cooling curves. Abscissae are time in minutes, ordinates are temperature in degrees C.

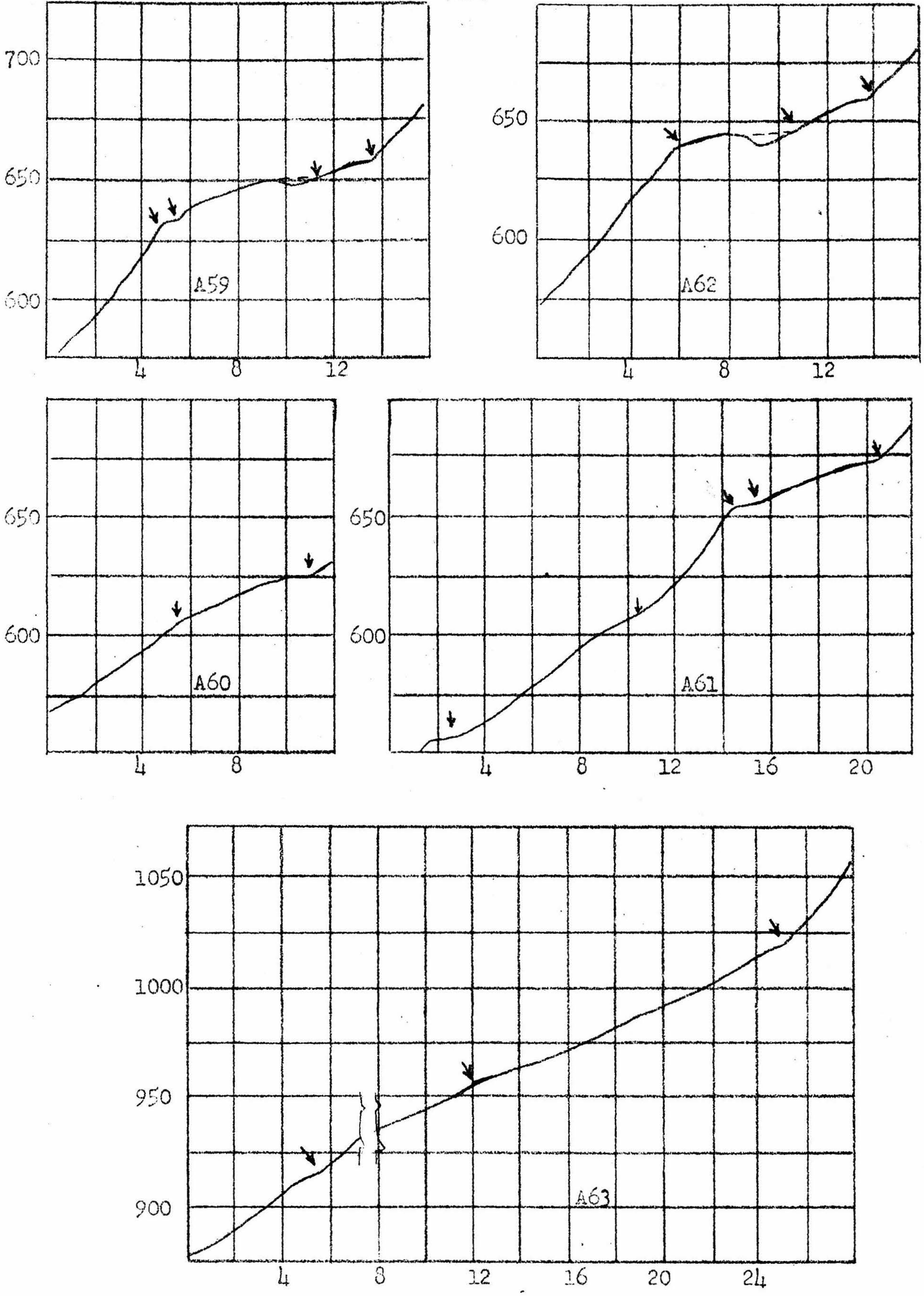

Fig. 19. Alloy cooling curves. Abscissae are time in minutes, ordinates are temperature in degrees C.

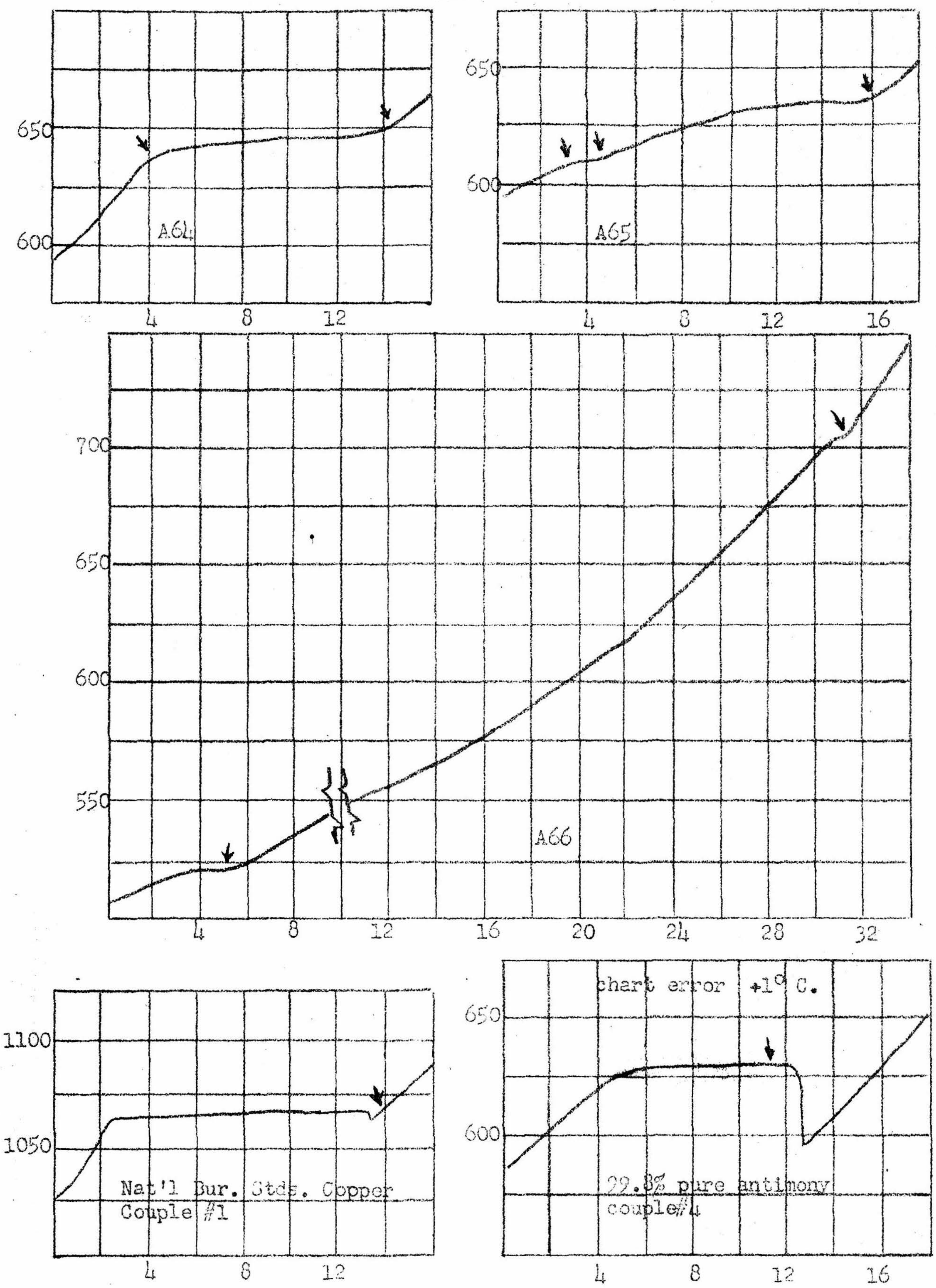

Fig. 20. Alloy cooling curves and cooling curves of copper and antimony. Abscissae are time in minutes, ordinates are temperatures in degrees C.

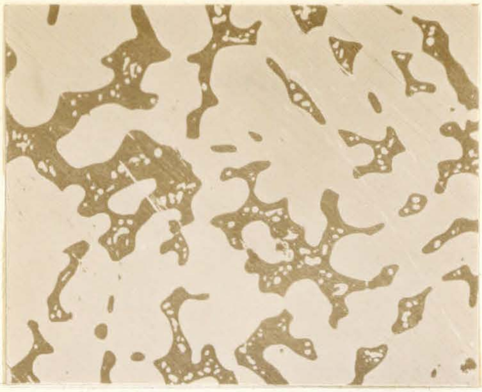

x140 $(NH_4)_2S_2O_8$

A4
(annealed 24 hrs.)

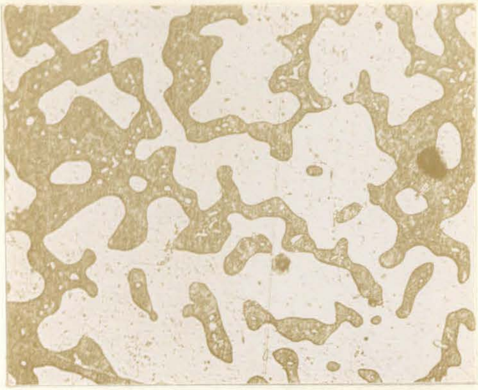

x140 $K_2Cr_2O_7$

A4
(annealed 48 hrs.)

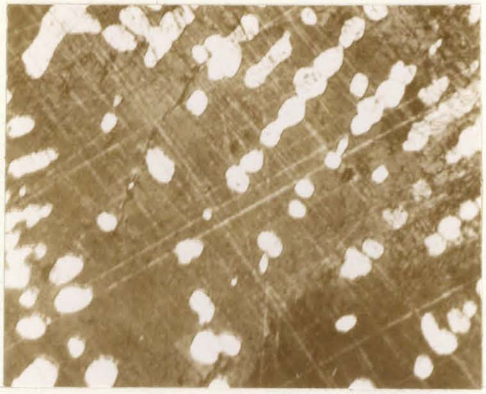

x75 $(NH_4)_2S_2O_8$

A17

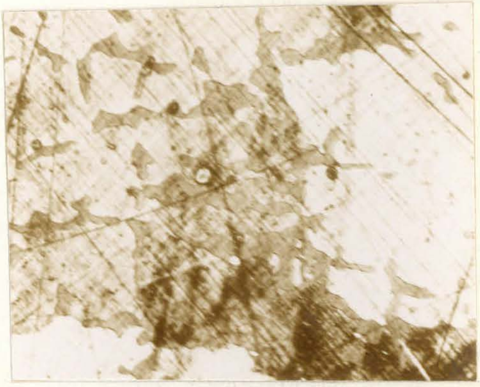

x75 $(NH_4)_2S_2O_8$

A20

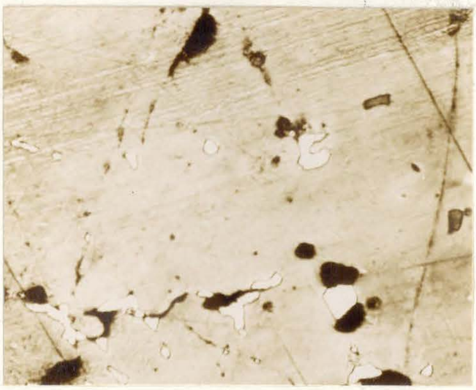

x75 $(NH_4)_2S_2O_8$

A21

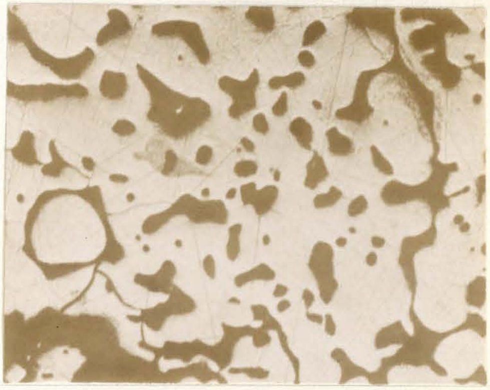

x50 $K_2Cr_2O_7$

A22

Fig. 21. Microphotographs of annealed and quenched Alloys.

x65 $(NH_4)_2S_2O_8$

A32

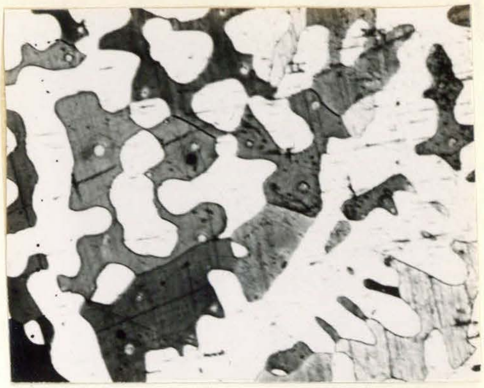

x75 $(NH_4)_2S_2O_8$

A33

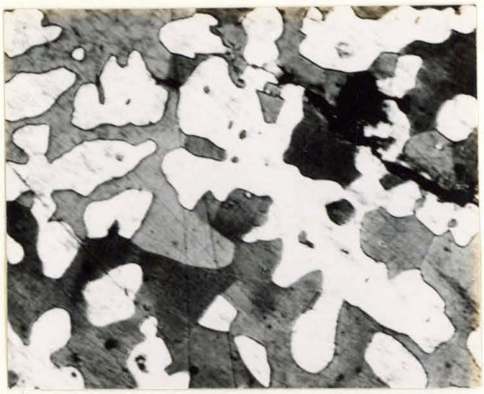

x75 $(NH_4)_2S_2O_8$

A36

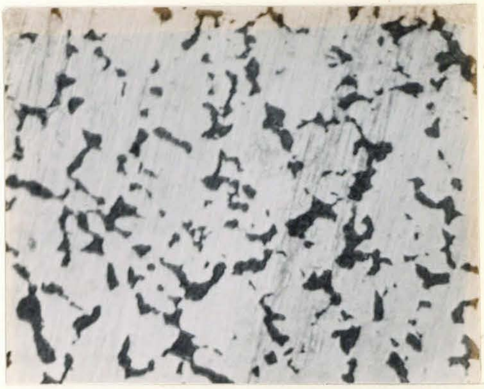

x75 $K_2Cr_2O_7$

A39

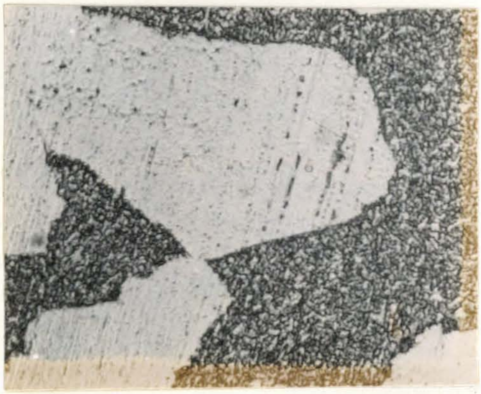

x860 $K_2Cr_2O_7$

A39

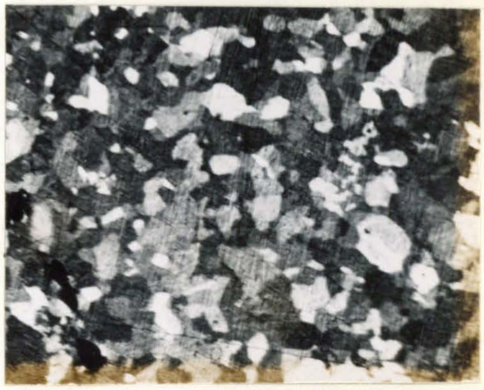

x75 $(NH_4)_2S_2O_8$

A41

Fig. 22. Microphotographs of Annealed and Quenched Alloys.

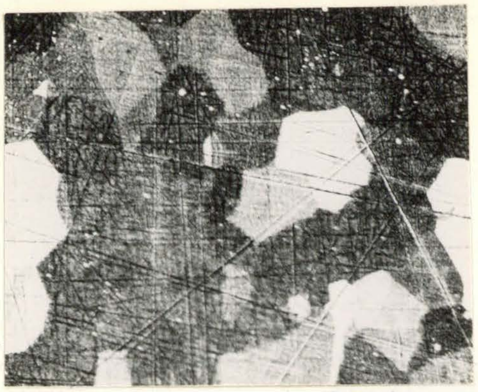

x300 $(NH_4)_2S_2O_8$

A41

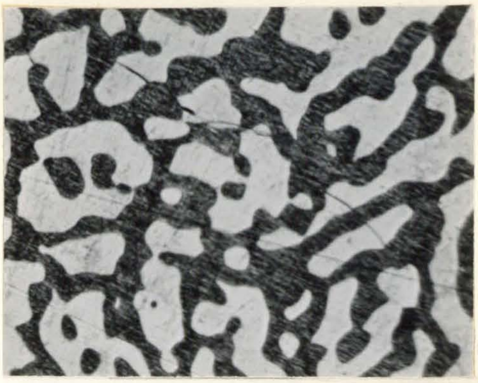

x75 $K_2Cr_2O_7$

A43

x1000 $K_2Cr_2O_7$

A43

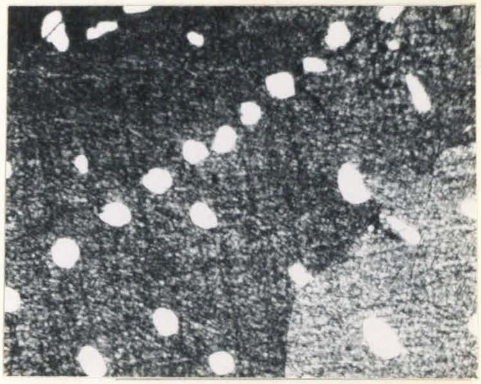

x75 $(NH_4)_2S_2O_8$

A45

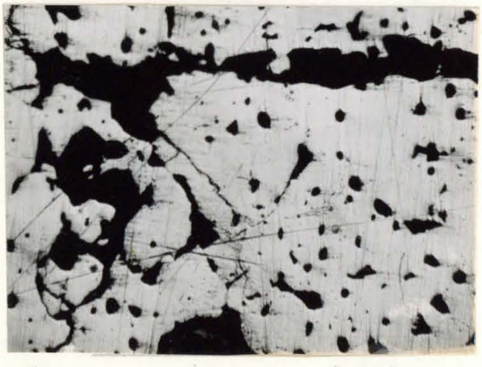

x50 $(NH_4)_2S_2O_8$

A49

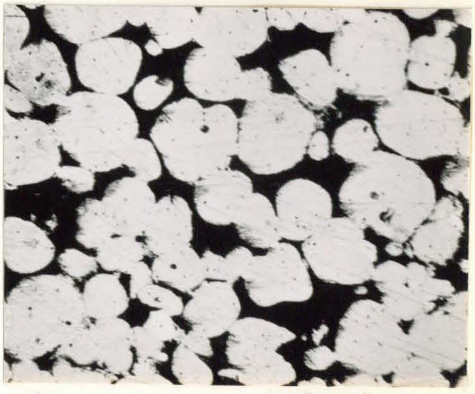

x50 $(NH_4)_2S_2O_8$

A50

Fig. 23. Microphotographs of Annealed and Quenched Alloys.

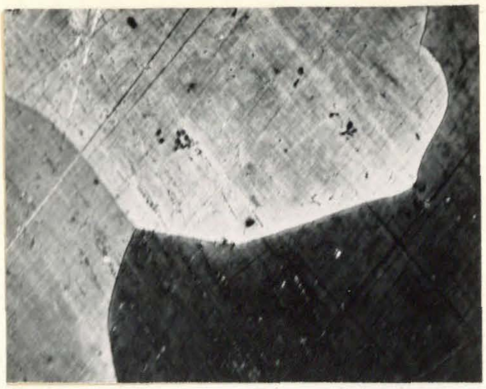

x75 $(NH_4)_2S_2O_8$

A51

x75 $K_2Cr_2O_7$

A52

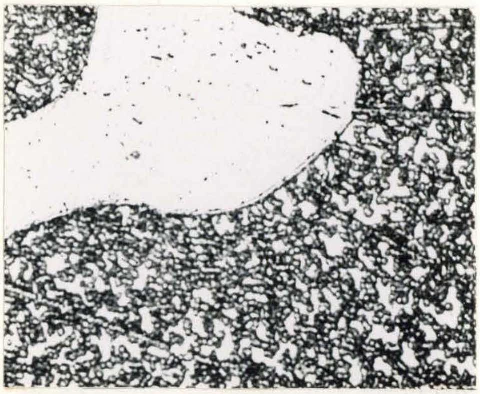

x1000 $K_2Cr_2O_7$

A52

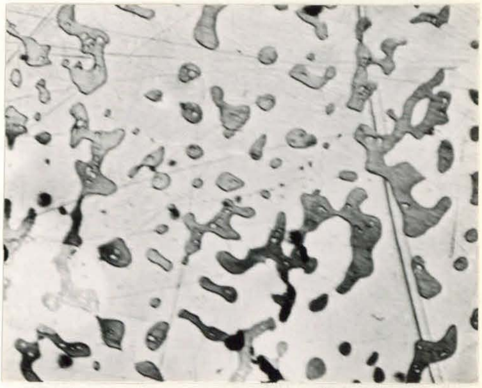

x75 $(NH_4)_2S_2O_8$

A55

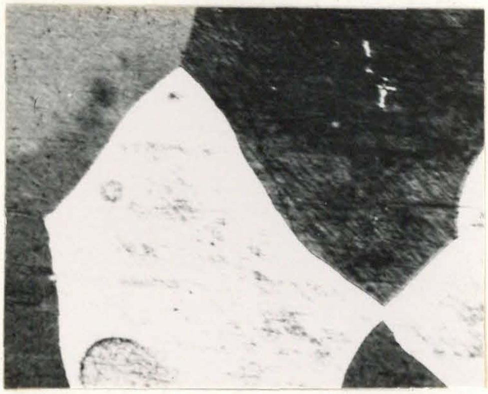

x75 $(NH_4)_2S_2O_8$

A56

x75 $(NH_4)_2S_2O_8$

A57

Fig. 24. Microphotographs of Annealed and Quenched Alloys.

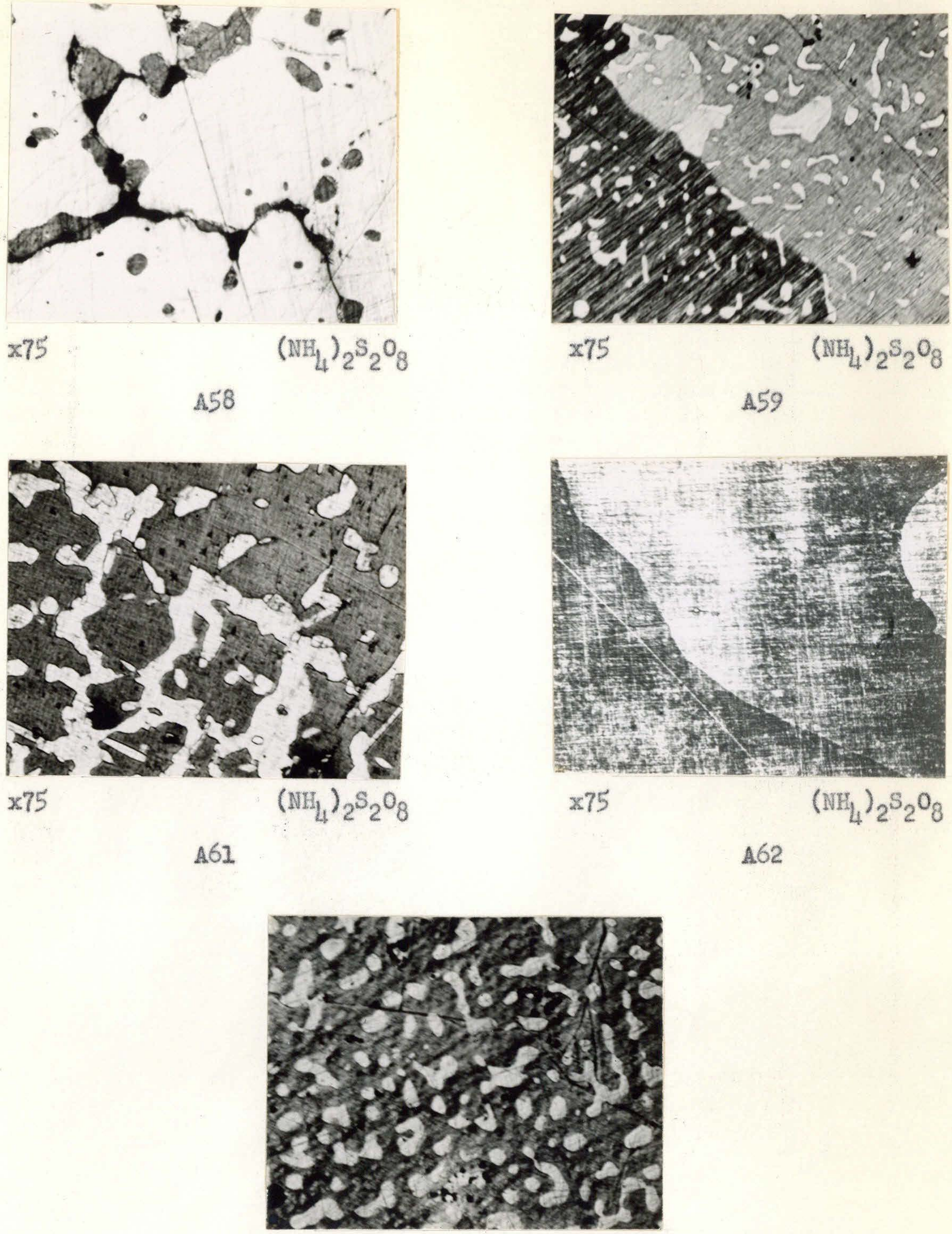

x75 $(NH_4)_2S_2O_8$

A58

x75 $(NH_4)_2S_2O_8$

A59

x75 $(NH_4)_2S_2O_8$

A61

x75 $(NH_4)_2S_2O_8$

A62

x75 $(NH_4)_2S_2O_8$

A65

Fig. 25. Microphotographs of Annealed and Quenched Alloys.

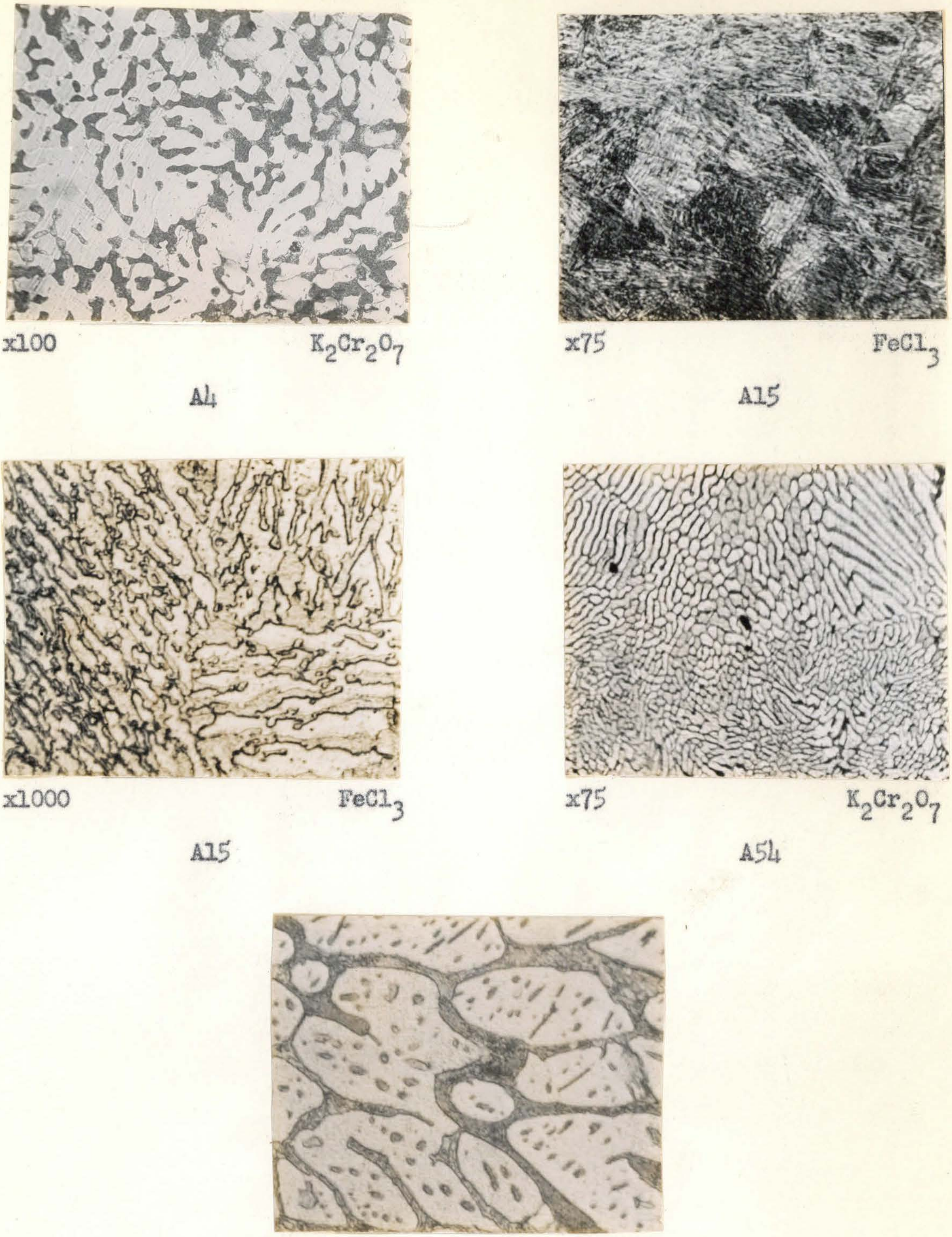

x100 $K_2Cr_2O_7$

A4

x75 $FeCl_3$

A15

x1000 $FeCl_3$

A15

x75 $K_2Cr_2O_7$

A54

x1000 $K_2Cr_2O_7$

A54

Fig. 26. Microphotographs of Unannealed Alloys.

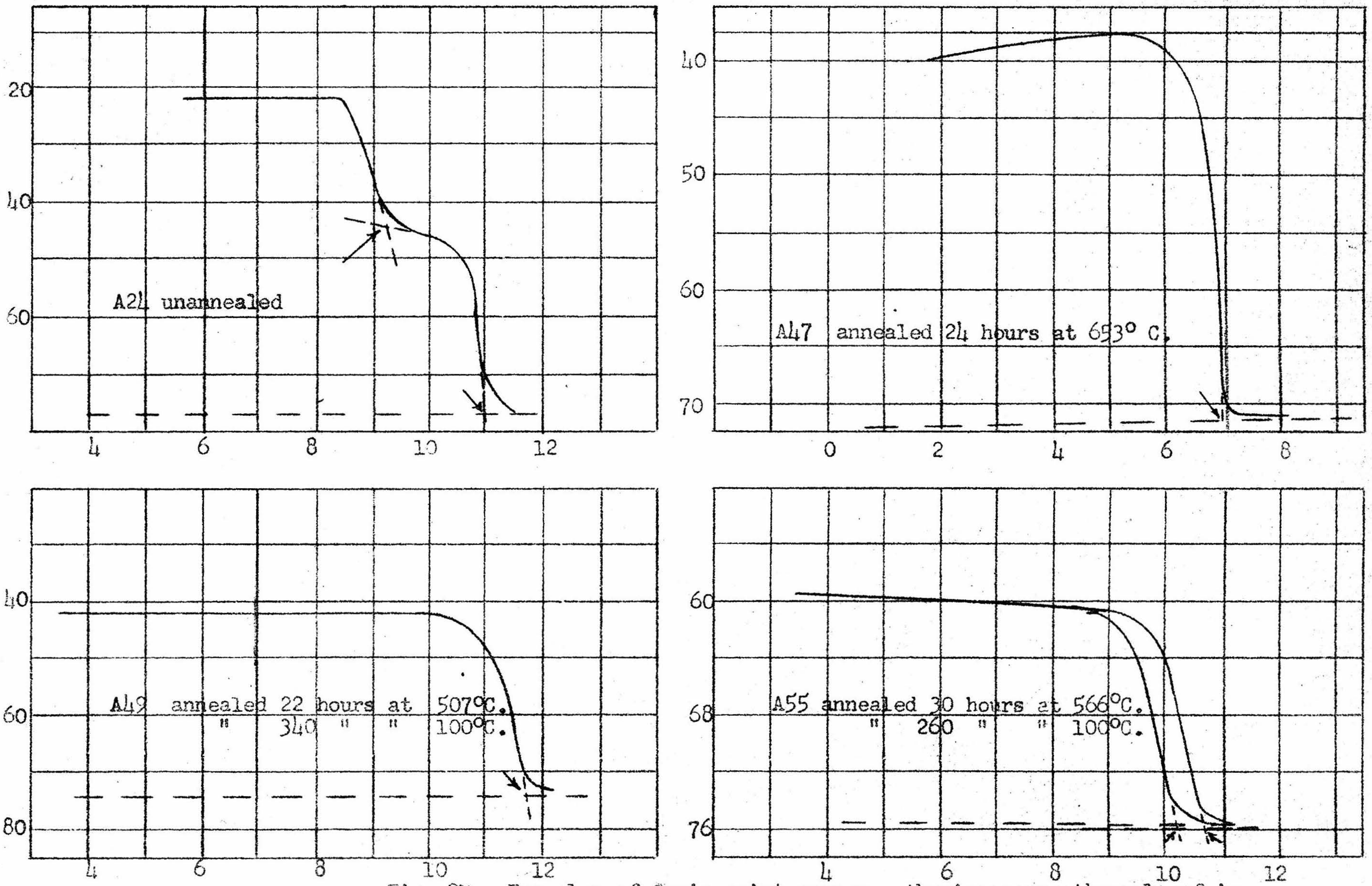

Fig. 27. Examples of Curie point curves. Abscissae are thermal emf in millivolts, ordinates are scale deflection in centimeters.

Figures are curie temperatures in degrees C. "RT" indicates a curie point lower than room temperature.

Fig. 28. Curie point contours of freshly quenched alloys.

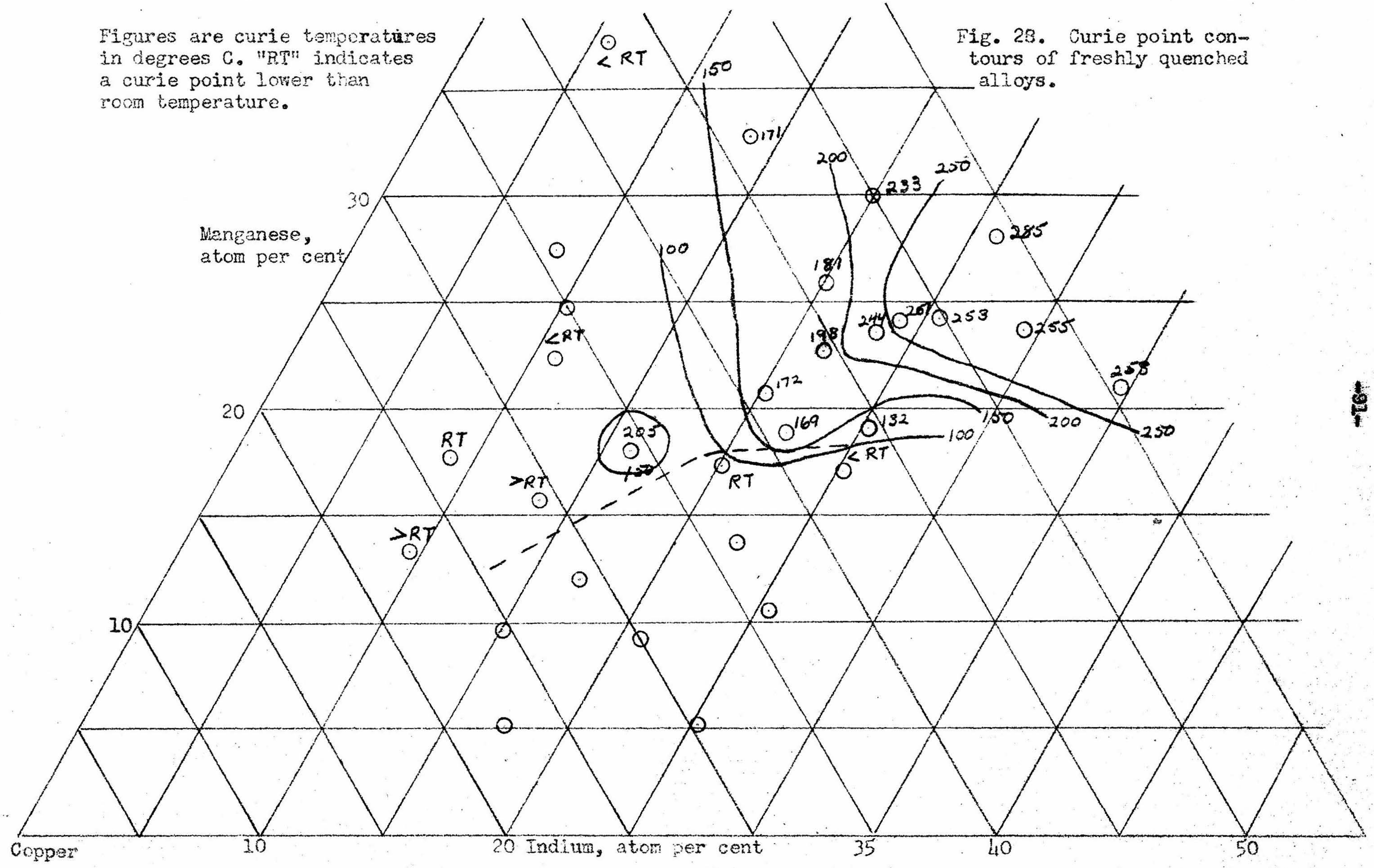

Figures are curie temperatures in degrees C. "RT" means room temperature.

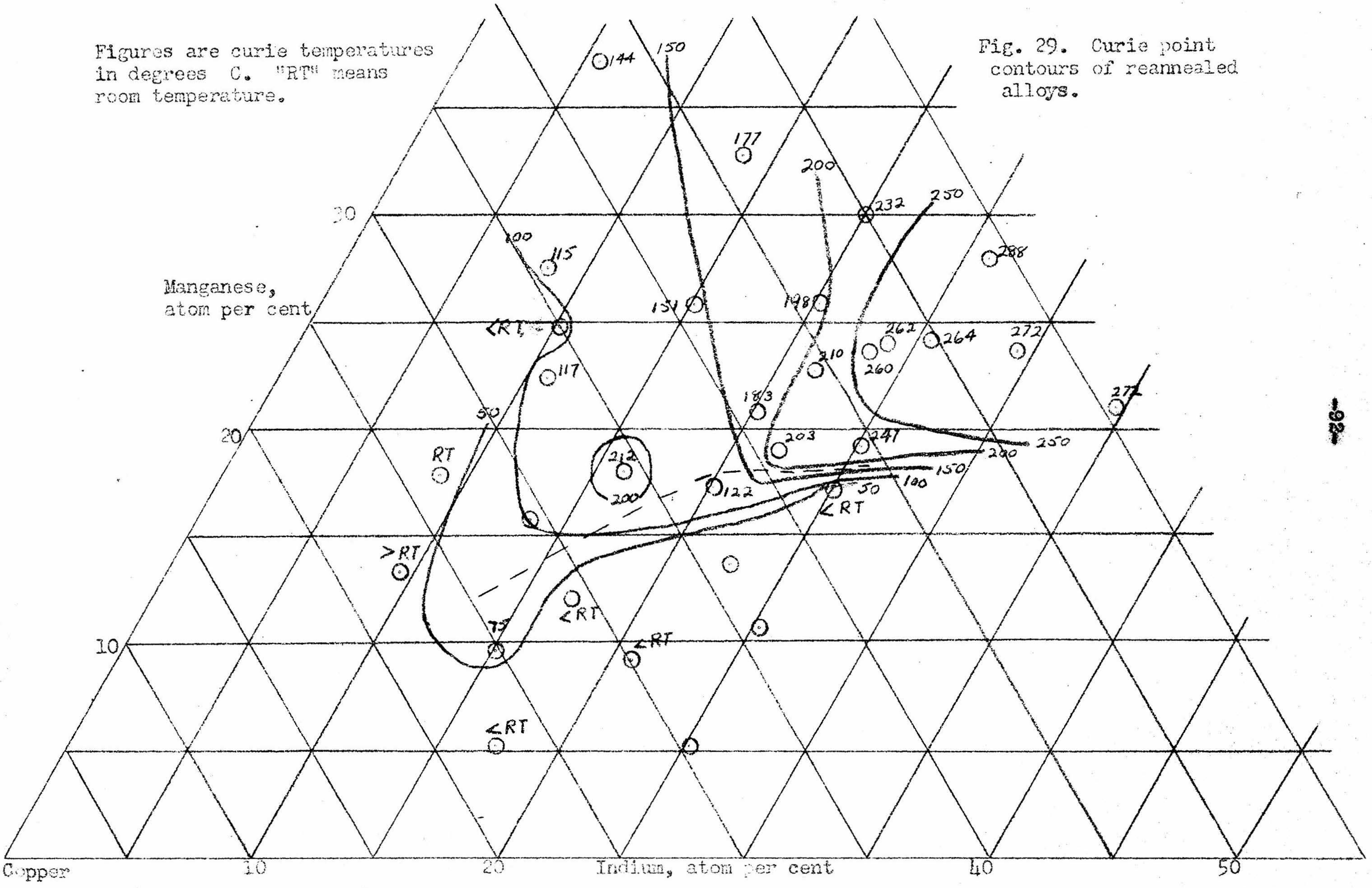

Fig. 29. Curie point contours of reannealed alloys.

Figures are curie temperatures in degrees C.

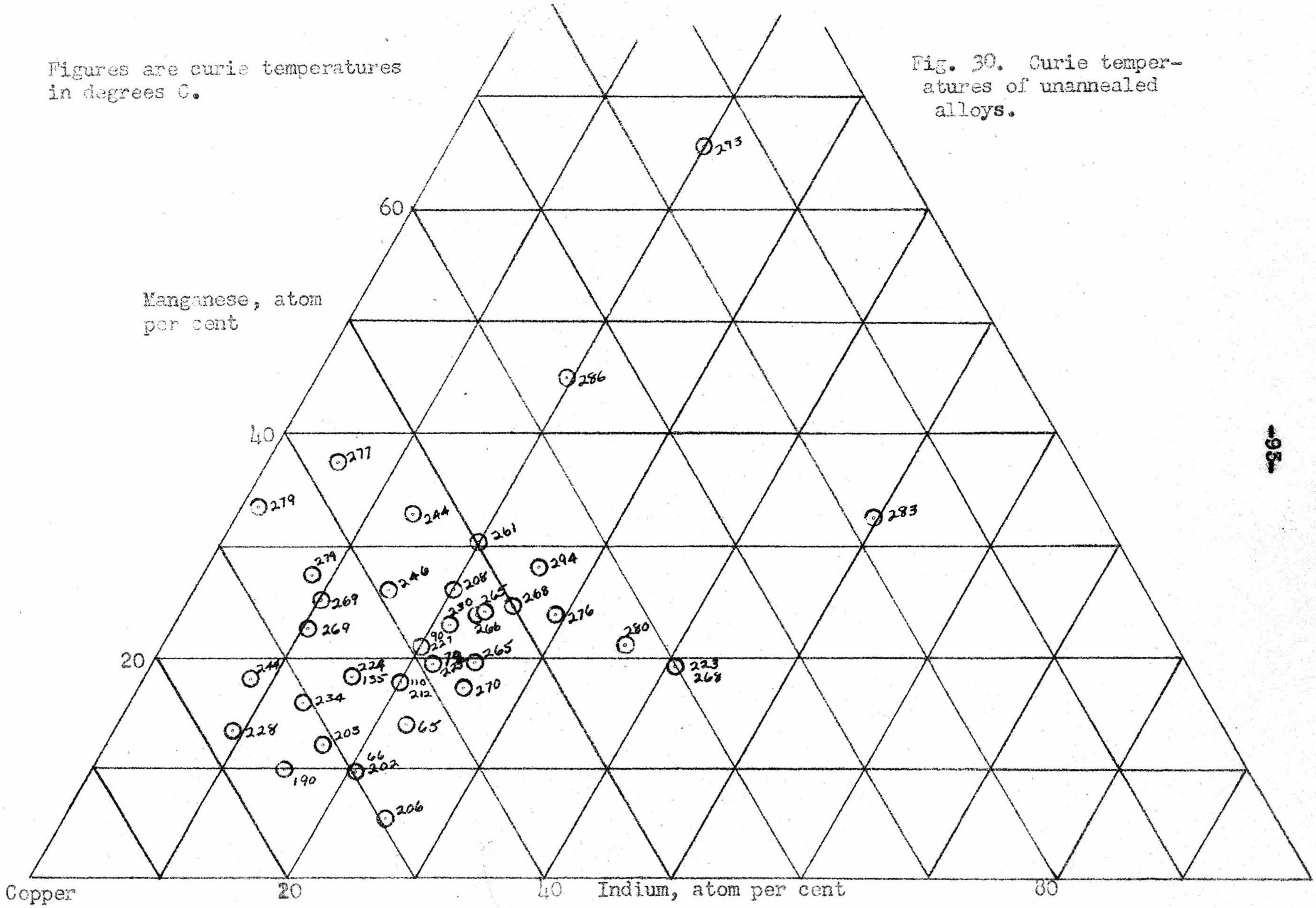

Fig. 30. Curie temperatures of unannealed alloys.

PROPOSITIONS

1. The principle of the orthicon television tube could be applied to electron diffraction work, enabling intensity variations of the scattering pattern to be converted to electrical quantities.

Rose & Iams, RCA Rev. 4, 186, (1939)

2. Electrolytic capacitors of increased capacity might be made by forming the dielectric film on a titanium or titanium-barium surface. It is possible that the film might be composed of the high dielectric constant materials TiO_2 or $BaTiO_3$.

Bunting, Shelton & Creamer, J. Res. Nat. Bur. Stds. 38, 337, (1947)
Wainer, Trans. Am. Electrochem. Soc. 89, 331, (1946)

3. Curie temperatures of ferromagnetic substances could be measured by a method which uses the specimen as the core of a coil in an oscillating electrical circuit. When the Curie point is reached, the decrease of magnetic permeability of the sample from a large value to one, the paramagnetic value, could be observed by recording the values of any one of a number of electrical quantities in the oscillating circuit.

4. Results of various workers on the electrolytic reduction of pentavalent columbium in sulfuric acid solutions are difficult to in-interpret, especially in regard to the linking of the various colors to the oxidation states involved. Assumption of a series of mixed oxidation states may account for the facts. Experiments are proposed which should help clarify the situation.

Golibersuch & Young, J.A.C.S. 71, 2402, (1949)
Kiehl & Hart, J.A.C.S. 50, 1608, (1928)
Kiehl, Fox & Hardt, J.A.C.S. 59, 2395, (1937)

5. Wada & Ishii have found that indium is extracted quantitative-

ly from 4.5 N HBr solutions by ether. This could be made the basis of a volumetric determination of indium.

Wada & Ishii, Sci. Papers Inst. Phys. & Chem Rsch. of Tokyo 34, 787, (1938)

6. The solubility of indium iodate in nitric acid solutions rises to a sharp maximum at about 5 N acid, then decreases to a very low value in 14 N acid.

a. The initial increase is explainable on the basis of the formation of undissociated iodic acid, but the subsequent decrease must due to some other cause.

b. It is proposed that the solid phase in this second region is either pure indium nitrate or a double salt containing both iodate and nitrate.

c. One test of this proposal would be to determine the solubility of indium nitrate in nitric acid solutions.

Ensslin, Zeit. f. Anorg. & Allgem. Chemie 250, 199, (1942)

7. In the Cu-In, Cu-Al and Cu-Ga equilibrium diagrams, the structures of the γ phases are as yet undetermined, since they cannot be retained by quenching, although their low-temperature modifications are known in each case to have the γ brass type of structure.

a. It is proposed that, due to the apparent speed with which these transitions take place, they are not polymorphic transitions, but possibly an order-disorder type.

b. The high-temperature x-ray method of Hume-Rothery & Reynolds could be used to determine these structures.

Am. Soc. Metals Handbook, 1948 ed.
Hansen, "Aufbau der Zweistofflegierungen", Springer, Berlin
Laves & Wallbaum, Zeit. f. Angew. Mineral. 4, 17, (1942)
Hume-Rothery & Reynolds, Proc. Roy. Soc. A167, 25, (1938)

8. The following data are known for some of the Heusler-type alloys, all having the same body-centered cubic superlattice:

Alloy	Curie point	Bohr magnetons per Mn atom	Internuclear separation of Mn atoms (Å)	Ratio: $\frac{\text{internucl. sep'n.}}{\text{diam. Mn 3d shell}}$
Cu_2MnAl	450° C.	4.04	4.19	2.44
Cu_2MnIn	264° C.	4.04	4.38	2.56
Cu_2MnSn	—	4.14	4.36	2.55

It will be noted that the values in column 3 are the same for the Al and In alloys, while the curie point of the latter is considerably the lower.

a. It would be interesting to obtain similar data for Cu_2MnGa and Cu_2MnB, providing the same type of structure exists in these alloys, and to see whether the same statements can be applied to all four alloys.

b. Another suggested set of experiments would be to determine the same quantities for analogous alloys, using as the third element Si, Ge and Pb, or Be, Mg, Zn or Cd. Some of these alloys are already known to be ferromagnetic, and the point to be examined here is whether the 4th group elements all increase the apparent magnetic moment of the manganese atom, and whether the 2nd group elements decrease it.

Slater, Phys. Rev. 36, 57, (1930)
Coles, Hume-Rothery & Myers, Proc. Roy. Soc. A196, 125, (1949)
Heusler, Ann. d. Phys. 19, 155, (1934)
Carapella & Hultgren, Metals Technology, T. P. 1405, (Oct. 1941)
Present Thesis

9. An explanation of the large increase in acid strength of benzoic acid produced by ortho-substituted halogens has been given by Jenkins, by attributing it to the direct effect of the dipole field. Hydrogen bonding does not appear to play a part, although in view of the geometry of the molecules, it seems rather surprising that it does not. An examination of the infra-red spectra of these molecules

should throw some light on this question.

Jenkins, J. Chem. Soc. (1939), 640

10.a. It is proposed that an improved modification of the well-known crossword puzzle could be constructed using triangular co-ordinate paper of the type used in ternary equilibrium work, thus providing tri-directional freedom of motion.

b. It is proposed that an additional qualifying examination, to be conducted by a suitably qualified faculty committee, be given incoming graduate students in chemistry to determine their aptitude in the field of baseball.